

EXA 12

2712

# NATIONAL ADVISORY COMMITTEE FOR AERONAUTICS

TECHNICAL NOTE 1892

POSITION ERRORS OF THE SERVICE AIRSPEED  
INSTALLATIONS OF 10 AIRPLANES

By William Gracey

Langley Aeronautical Laboratory  
Langley Air Force Base, Va.

Reproduced From  
Best Available Copy



Washington

June 1949

**DISTRIBUTION STATEMENT A**  
Approved for Public Release  
Distribution Unlimited

20000731 181

DTIC QUALITY INSPECTED 4

AQM00-10-3350

NATIONAL ADVISORY COMMITTEE FOR AERONAUTICS

TECHNICAL NOTE 1892

POSITION ERRORS OF THE SERVICE AIRSPEED  
INSTALLATIONS OF 10 AIRPLANES

By William Gracey

SUMMARY

Calibrations of the static-pressure or "position" errors of the service airspeed installations of 10 present-day airplanes are presented. The installations are representative of most of the systems in use at the present time and include static-pressure vents on the nose and the rear section of the fuselage and pitot-static tubes mounted on the wing, the vertical tail, and the nose of the fuselage.

Each of the installations was calibrated under steady flight conditions by means of a trailing static-pressure tube. The tests were conducted from speeds near the stall to maximum indicated speeds not exceeding 260 miles per hour. Calibrations of representative flight conditions (climb, glide, wave-off, and landing) were obtained in order to show the variation of static-pressure error with engine power and flap setting. The position errors for the various flight conditions are presented as static-pressure errors and as airspeed and altitude errors.

Analysis of the data presented showed that the static-pressure error for static vents on the rear section of the fuselage remained approximately constant with angle of attack and became more negative with flap deflection. The static-pressure errors for the wing, fuselage-nose, and vertical-tail installations became more negative with increasing angle of attack and more positive with flap deflection; the effect of engine power for these installations followed no consistent trend.

INTRODUCTION

The pressure registered by the static-pressure tube of an airspeed installation will, as a general rule, differ appreciably from free-stream static pressure. For the usual case the magnitude of the static-pressure error will depend on the type of tube employed, on the location of the tube in the pressure field surrounding the airplane, and on the alinement of the tube with the local air flow. The combined effect of these variables on the static pressure registered by the instruments is most readily determined by calibrating the installation in flight. Since the

value of the static-pressure error depends for the most part on the location of the tube in the pressure field, the over-all error obtained from the flight calibration has come to be known as the "position" error of the static tube.

Attempts to discover suitable locations for service installations employing pitot-static tubes have been made by theoretical, wind-tunnel, and flight investigations. (See references 1 to 3.) These tests have shown that three wing installations (0.4 chord ahead of the leading edge, above and to the rear of the trailing edge, and below and to the rear of the under surface) will provide velocity errors of less than 5 percent throughout the speed range. These installations cannot always be employed, however, because of other factors (such as drag, icing, maintenance handling, pressure-tubing lag) that must be considered in the design of a given installation.

Similarly, satisfactory locations for service installations employing static-pressure vents installed on the sides of the fuselage have been determined for specific airplanes by both wind-tunnel and flight investigations. (See references 4 and 5.) The results of these tests have shown that for airplanes of conventional design two areas (on the fuselage nose ahead of the wing and on the rear fuselage between the wing and horizontal tail) will ordinarily prove satisfactory for the location of the vents. These positions may not be applicable to all airplanes, however, because of the presence of local protuberances or the shape of the fuselage in these regions. In any case, the location of the vents is ordinarily so critical that the most satisfactory position for a given airplane must be chosen on the basis of exploratory tests, either in wind tunnels or in flight, of several promising vent positions.

The service airspeed installations of present-day airplanes vary widely with regard to the location of the static-pressure sources. Pitot-static tubes, for example, are mounted ahead of the wing (in line with, above, and below the wing chord), below the wing, on the nose of the fuselage, and on the vertical tail; whereas static-pressure vents are located on the fuselage near the nose and between the wing and the horizontal tail.

Airplanes incorporating a relatively wide variety of these installations have been assigned to the Langley Laboratory during the past few years. Since a comparison of the position errors of various service installations was felt to be of general interest, the calibrations of the 10 representative static-pressure systems are presented herein. Although the calibrations of some of the installations are probably already known, the results of this investigation are believed to be more directly comparable, because each calibration was obtained by the same method and with the same instrumentation.

## SYMBOLS

$p_s$	free-stream static pressure
$p_s'$	pressure registered by static tube of service airspeed system
$\Delta p$	static-pressure or position error $(p_s' - p_s)$
$q_c'$	indicated impact pressure, inches of water
$c$	wing chord, inches
$t$	wing thickness, inches
$b$	wing span, inches
$x$	distance of static orifices ahead of wing leading edge, inches
$y$	distance of static orifices from wing chord, inches
$z$	distance of static orifices from wing tip, inches
$\rho_0/\rho$	density ratio

## TESTS

The scope of the tests includes calibrations of the airspeed installations of the airplanes shown in figures 1 to 10. These installations include eight pitot-static tubes (five on the wing, one on the vertical tail, and two on the nose of the fuselage) and two fuselage static-pressure vents (one near the nose and one between the wing and horizontal tail). The locations of the static-pressure orifices of the pitot-static tubes mounted on the wing are given in table I, and those of the remaining installations are shown in figures 11 to 15.

The calibrations were determined in each case by means of a trailing static-pressure tube (reference 6) over a speed range from speeds near the stall to maximum indicated speeds not exceeding 260 miles per hour (the speed at which the trailing tube becomes unstable). Each installation was calibrated for two or more of the following flight conditions:

Flight condition	Flap and landing-gear setting	Engine power
Climb	Retracted	Normal rated
Glide	Retracted	Engine idling
Wave-off	Extended	Normal rated
Landing	Extended	Engine idling

The static-pressure errors were determined by measuring the differential pressure between the trailing tube and the static system of the airplane. This differential pressure was recorded by an NACA airspeed recorder having a range from -1 to 3 inches of water. The trailing tube employed for these tests has a correction factor of one-half of 1 percent of the impact pressure.

The type of tube employed in the various pitot-static installations is noted in table I and figures 11 to 13. Details of the two static-vent installations are shown in figures 9 and 10. In those cases where the installations comprised two pitot-static tubes or two static vents, the two static sources were combined to give average indications.

### RESULTS AND DISCUSSION

The results of the tests are presented in figures 16 to 26. The symbol  $\Delta p$  denotes the static-pressure or position error and is defined by the relation  $\Delta p = p_s' - p_s$ , where  $p_s'$  is the pressure registered by the static head of the service airspeed system and  $p_s$  is the free-stream static pressure. This error is expressed as a fraction  $\Delta p/q_c'$  of the indicated impact pressure  $q_c'$  and is plotted against  $1/q_c'$ , which is proportional to the lift coefficient for the low speeds considered.

The position errors of the various installations are also presented in terms of airspeed errors and altitude errors (for sea-level conditions) as functions of the indicated airspeed (figs. 27 to 36). These charts were prepared from the curves in figures 16 to 20 and 22 to 26.

Although the static-pressure error has been expressed as an error in airspeed, it should be noted that these velocity errors will be valid only if no error exists in total pressure. For the usual installation the total-pressure tube will indicate correctly, except for a relatively small error caused by the drain hole (reference 7). However, when a total-pressure tube is located in a region where the flow direction changes markedly with angle of attack (as, for example, near the leading edge of a wing or the nose of a fuselage), the pressure developed by the tube will be in error at high angles of attack (reference 8). Since the static pressure will ordinarily be lower than free-stream static pressure at high angles of attack, the two errors will tend to compensate so that the resulting velocity error will be less than that ascribed to the static-pressure error alone. For those cases in which the static-pressure error is positive at high angles of attack, the total and static errors will, of course, be additive.

The altitude-error curves, on the other hand, represent the actual errors that will be introduced in the altimeter indications for standard sea-level conditions. These errors will increase with altitude in accordance with the ratio  $\rho_0/\rho$ .

Although the results of the tests do not lend themselves to rigid analysis, an understanding of the relative magnitudes and trends of the various calibrations may be derived from a consideration of the pressure fields about the wings and fuselage.

### Static-Pressure Systems on Wings

For the purpose of this discussion the pressure field in front of a wing may be considered to consist of a region directly ahead of and below the leading edge in which the pressures are greater than free-stream static pressure and, somewhat above this region, a second region in which the pressures are less than stream pressure. Within each of these regions the magnitude of the static pressure will vary from point to point, the exact pressure distribution depending on the shape and thickness of the airfoil (reference 9). Except in the vicinity of the leading edge of the wing, the pressures along vertical lines increase progressively from the low to the high pressure regions; the pressure along the contour dividing the two regions is thus equal to stream pressure. In the high pressure region the static pressure is greatest at the leading edge of the wing, decreases rapidly within a relatively short distance, and approaches free-stream pressure at 1 or 2 chords ahead of the wing. As the angle of attack of the wing is increased, the contour of zero pressure defect moves downward toward the extension of the chord line of the wing. A static tube extending from the leading edge of the wing, therefore, moves from a region of high pressure to one of lower pressure as the angle of attack increases. Any misalignment of the tube with the local air flow will, of course, cause a further decrease in the pressure registered by the tube. For these reasons the static-pressure error changes from positive to negative as the stalling speed is approached. (See figs. 16 to 20.)

A comparison of the calibrations of the five wing installations based on the position errors at low angles of attack (fig. 21) provides an indication of the magnitude of the static-pressure error as a function of the position of the tube with respect to the leading edge of the wing. This comparison is, of course, approximate in that no account has been taken of the difference in shape of the various wing sections, the position of the tube along the span, or the position of the tube with respect to the extension of the chord line of the wing. Note, however, that similar installations on different types of airplanes exhibit nearly the same position errors. The static tubes of airplanes B and C, for example, are located in approximately the same position with respect to the leading edge of the wing and to the extension of the chord line; the static-pressure error in each case is about 5 percent  $q_c'$ , even though the spanwise position of the tubes is quite different. For purposes of comparison, pertinent data from the wind-tunnel tests of reference 3 have also been plotted in figure 21.

The magnitude of the position error as a function of the position of the tube with respect to the chord line may be shown from a comparison of the static-pressure errors of installations A and D (fig. 21). These data show that the error may be decreased when the tube is located above the chord line. This advantage, however, is offset by somewhat larger errors at the stalling speed, a fact indicating that a tube mounted above the chord line moves farther into the low pressure region at high angles of attack. By the same reasoning, the static-pressure error of a tube mounted below the chord line should be relatively small at high angles of attack. Supporting evidence for this assumption may be found in the calibration of airplane D, for which the error at the stall is less than 5 percent  $q_c'$ . (See fig. 19.) The installation on airplane E, on the other hand, exhibits large negative errors in the low speed range even though the tube is located below the chord line. (See fig. 20.) This apparent discrepancy may be explained by the fact that the airspeed tube is located near the leading edge of the wing where the induced angle of attack becomes appreciable, especially at the higher lift coefficients. Under these conditions the effective or actual angle of attack at the tube is the sum of the angle of attack of the wing and the angle of attack induced by the wing. The pressure registered by the tube will, therefore, be more negative because of the greater misalignment with the local air flow.

The effects of flap setting and engine power on the position errors of the wing installations may be seen from a comparison of the calibrations under different flight conditions. (See figs. 16 to 20.) Examination of these curves will show that, for a given dynamic pressure, the static-pressure error becomes more positive when the flaps are deflected. This characteristic may be explained from the fact that, for a fixed value of lift coefficient (or  $l/q_c'$ ), the angle of attack of a wing decreases as the flaps are deflected. Since the position error for the flaps-up condition becomes more positive with decreasing angle of attack, the position error for the flaps-down condition will, therefore, be more positive than that for the clean condition at the same impact pressure. Figure 20 shows, however, that even though the effect of flap setting of airplane E at speeds near the stall is the same as the other wing installations, the trend is reversed at somewhat higher speeds. The reason for this discrepancy is difficult to explain on the basis of existing information on pressure fields surrounding airfoils. The data in reference 9, however, do show that in the vicinity of the wing leading edge (especially in that region occupied by the tube on airplane E) the pattern of pressure contours is concentrated and more complex than that forward of the wing. Any disturbance in the pressure field, therefore, such as that caused by flap deflection, could presumably result in pressure changes at the leading edge which would differ from changes occurring ahead of the wing.

The effect of engine power on the static-pressure errors is seen to follow no consistent trend. Power effects for installations D and E, for example, are appreciable but with opposite sign, whereas the effect of power for airplanes A, B, and C is negligible. The reason for these

differences may be attributed to the angle-of-attack changes that result from the application of power and to the accompanying changes in lateral and directional trim. The effects of these three factors vary both in sign and magnitude and may be either additive or compensating, depending on the configuration of the airplane-power-plant arrangement and on which wing the airspeed tube is located. That the effect of power on the static-pressure errors of somewhat similar installations varies considerably from one airplane to another may therefore be readily seen.

### Static-Pressure Systems on Forward Section of Fuselage

An insight into the nature of the calibrations of the static-pressure systems on the forward section of a fuselage may be obtained from a consideration of the pressure distribution about a body of revolution having an elliptical nose shape. A theoretical analysis for a body of this shape at zero angle of attack (reference 10) has shown that the pressure along the surface is greatest at the nose (the stagnation point), decreases rapidly to one-third of the dynamic pressure less than free-stream static pressure at approximately  $1/3$  body diameter behind the nose, and rises asymptotically thereafter to stream pressure. At 3 body diameters behind the nose the pressure is about 2 percent of the dynamic pressure below stream pressure. When the angle of attack of the body is increased, the stagnation point moves downward and back along the body. If orifices are located on the sides of the body and in the region of the pressure rise, that is, to the rear of the  $1/3$  diameter station, the pressure registered by the orifices will decrease (as the angle of attack is increased) because the distance from the orifices to the stagnation point is effectively decreased. The effect is the same as if the body remained at zero angle of attack and the orifices were moved toward the nose.

Of the three fuselage-nose installations, that of airplane I is the only one affording an opportunity for direct comparison with theory, because in this case the fuselage is circular, the nose shape is approximately elliptical, and orifices are employed as the static-pressure source. The static-pressure orifices, or vents, are located approximately  $1\frac{1}{2}$  body diameters to the rear of the nose. The theory indicates that the static-pressure error (at zero angle of attack) for this position should be about 8 percent  $q_c$  below stream pressure. If the high-speed climb condition can be considered as most nearly representing the condition for zero angle of attack, the static-pressure error (-6 percent  $q_c$ ) will be seen to compare favorably with the theoretical value. Similar comparisons cannot, of course, be made for installations G and H because pitot-static tubes are employed, the tubes project outward from the fuselage, and the fuselage nose shapes are not ellipsoidal. The tubes on both of these airplanes, however, are sufficiently close to the surface of the fuselage to be influenced by the presence of that body, because the static-pressure errors remain negative throughout the speed



range. That the position errors at large angles of attack for these installations are more negative than those for the static vents of airplane I is due to the proximity of the tubes to the nose of the fuselage and to the misalignment of the tubes with the local flow.

The effect of flap setting on the position error of each of the fuselage-nose installations is the same as that for pitot-static tubes mounted on the wing (that is, the static-pressure error becomes more positive when the flaps are deflected) and the cause of this effect is the same as that already noted in the discussion of the wing installations. The effect of engine power, like that for the wing installations, follows no consistent trend. Power effects for installations I and H, for example, are opposite and are quite large, whereas the effect of power on installation G is negligible.

#### Static-Pressure Systems on Rear Section of Fuselage

The characteristics of static-pressure vents on the rear section of a fuselage are exemplified by the calibration of installation J (fig. 26). In contrast to the fuselage-nose installations (where the static pressure at the vent is determined primarily by the pressure distribution over the fuselage) static-pressure vents on the rear section of the fuselage are subject to the effects of the fuselage, the wings, the horizontal tail, and, if the airplane is of the single-engine propeller-driven type, the propeller slipstream. In the absence of wing and tail surfaces, the pressure on the rear part of the fuselage should be very nearly stream pressure. Furthermore, the effect of the propeller slipstream should be relatively small. The magnitude of the static-pressure error, therefore, is determined largely by the combined effects of the pressure fields behind the wing and ahead of the horizontal tail. The pressure field behind the wing, like that ahead of the wing, consists of two distinct regions (reference 9). Directly to the rear and below the trailing edge the pressures are greater than stream pressure; above this region the pressures are less than stream pressure. When the angle of attack of the wing is increased, or when the flaps are deflected, the line of zero pressure defect moves downward toward the extension of the chord line of the wing. The pressure field ahead of the horizontal tail is similar to that ahead of the wing and changes with angle of attack in the same manner as the field ahead of the wing. The calibration of installation J can now be explained on the basis of the interaction of the pressure fields from the wing and tail. The fact that the static-pressure error is small and remains constant throughout the angle-of-attack range, for example, indicates that the orifices are located between the two contours of zero pressure defect where the errors arising from the two fields tend to compensate. Furthermore, the fact that the error becomes more negative with flap deflection (instead of more positive as in the case of the wing installations) can be explained from the large downward travel of the pressure field behind the wing when the flaps are deflected.

## Static-Pressure System on Vertical Tail

The characteristics of a static tube mounted on the vertical tail are shown by the calibration of the fin installation on airplane F (fig. 22). Despite the proximity of the tube to the leading edge of the fin, the static-pressure error at the higher speeds (for the climb condition) is relatively small (4 percent  $q_c'$ ), owing, apparently, to the fact that the tube extends beyond the tip of the fin.

The variation of position error with angle of attack is the same as that of the wing installations; that is, the error becomes more negative with increasing angle of attack. Since the pressure field at the vertical tail is determined primarily by angle of sideslip, however, the variation in position error with angle of attack is believed to result from misalignment of the tube with the local air flow. The effect of flap setting for this installation is the same as that for the wing installations, except that the magnitude of the effect is very much greater. Power effects are appreciable in the lower speed range, the application of power causing the error to become more positive.

## CONCLUSIONS

On the basis of calibrations of the static-pressure or "position" errors of the service airspeed installations of 10 present-day airplanes, the following conclusions have been reached:

1. The static-pressure error for wing, fuselage-nose, and vertical-tail installations becomes more negative with increasing angle of attack. The error for static vents located between the wing and horizontal tail remains approximately constant with angle of attack.
2. The static-pressure error for wing, fuselage-nose, and vertical-tail installations becomes more positive when the flaps are deflected. The error for the static-vent installation on the rear section of the fuselage becomes more negative with flap deflection.
3. The effect of engine power on the static-pressure error follows no consistent trend for any of the installations tested.

Langley Aeronautical Laboratory  
National Advisory Committee for Aeronautics  
Langley Air Force Base, Va., March 25, 1949

## REFERENCES

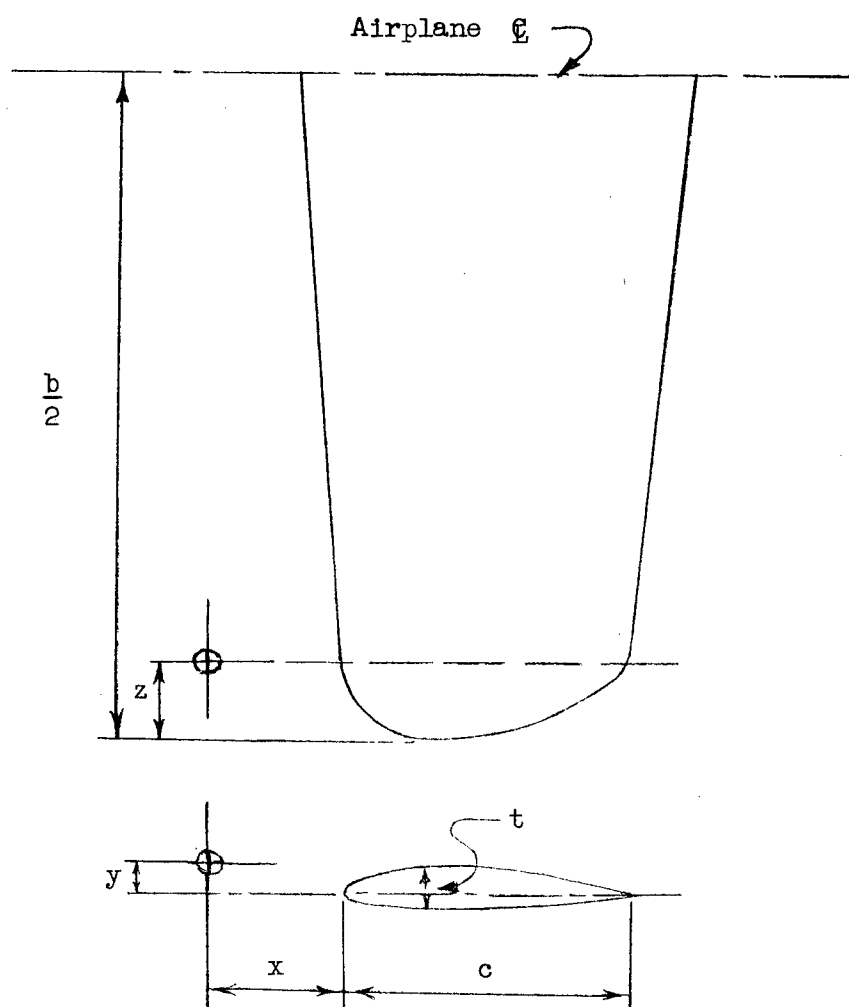
1. Gates, S. B., and Cohen, J.: Note on the Standardisation of Pitot-Static Head Position on Monoplanes. R. & M. No. 1778, British A.R.C., 1937.
2. Parsons, John F.: Full-Scale Wind-Tunnel Tests to Determine a Satisfactory Location for a Service Pitot-Static Tube on a Low-Wing Monoplane. NACA TN 561, 1936.
3. Lindsey, W. F.: Effect of Mach Number on Position Error as Applied to a Pitot-Static Tube Located 0.55 Chord Ahead of an Airplane Wing. NACA CB 14E29, 1944.
4. Scherrer, Richard, and Rodert, Lewis A.: A Flight Investigation of Fuselage Static-Pressure-Vent Airspeed Installations. NACA ARR 3K16, 1943.
5. Schoenfeld, L. I., and Harding, G. A.: Instructions for the Location, Installation and Calibration of Flush Static Vents. Rep. No. NAES-INSTR-15-44, NAF, Philadelphia Navy Yard, Bur. Aero., July 15, 1944.
6. Thompson, F. L.: The Measurement of Air Speed of Airplanes. NACA TN 616, 1937.
7. Thompson, F. L., and Zalovcik, John A.: Airspeed Measurements in Flight at High Speeds. NACA ARR, Oct. 1942.
8. Schoenfeld, L. I., and Harding, G. A.: Report on the Dual Sighting Stand and Other Methods of Calibrating Altimeter and Airspeed Installations. Rep. No. NAES-INSTR-16-44, NAF, Philadelphia Navy Yard, Bur. Aero., Aug. 15, 1944. (Issued July 1, 1945.)
9. Huston, Wilber B.: Accuracy of Airspeed Measurements and Flight Calibration Procedures. NACA TN 1605, 1948.
10. Kumbruch, H.: Pitot-Static Tubes for Determining the Velocity of Air. NACA TM 303, 1925.

TABLE I.- LOCATION OF STATIC-PRESSURE ORIFICES OF AIRSPEED TUBES  
 INSTALLED ON THE LEADING EDGE OF THE WINGS OF FIVE AIRPLANES

[Pitot-static tubes on all these airplanes were Kollsman type 369]

Airplane	c (in.)	t (in.)	b/2 (in.)	x (in.)	y (in.) (a)	z (in.)	x/c	y/t (a)	$\frac{z}{b/2}$	x/t
A	61	6.8	298	30	13	19	0.49	1.91	0.06	4.4
B	52	6.3	256	24	-.5	18	.46	-.08	.07	3.8
C	84	10.5	294	34.5	-2	102	.41	-.19	.35	3.3
D	60	5.0	249	21.5	-5.5	20	.36	-1.10	.08	4.3
E	63	5.7	257	5.5	-6.5	6.5	.09	-1.14	.03	1.0

<sup>a</sup>The sign of y is positive when the orifices are located above the chord.



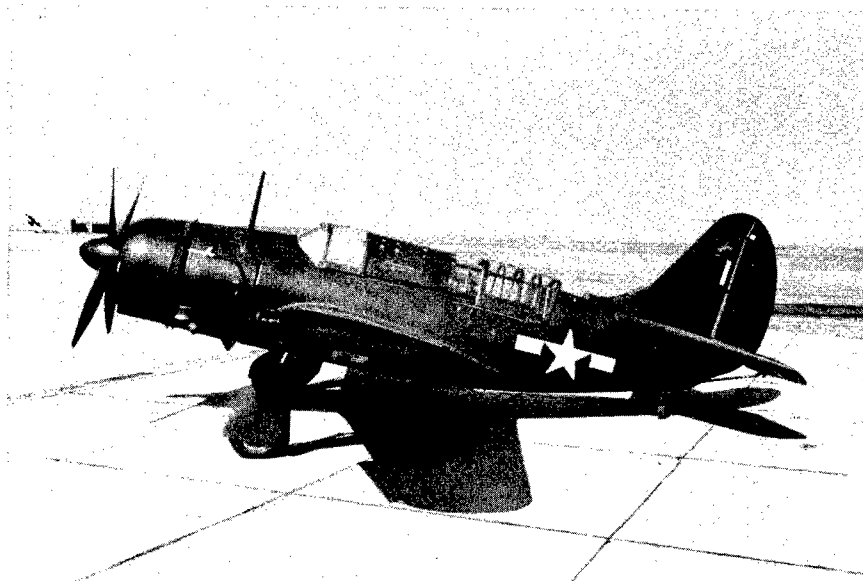


Figure 1.— Airspeed tube on airplane A.

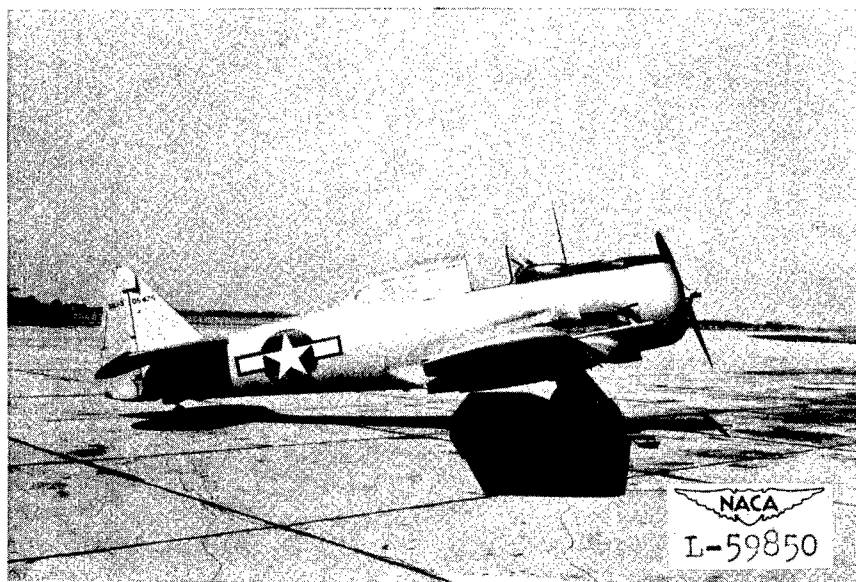


Figure 2.— Airspeed tube on airplane B.

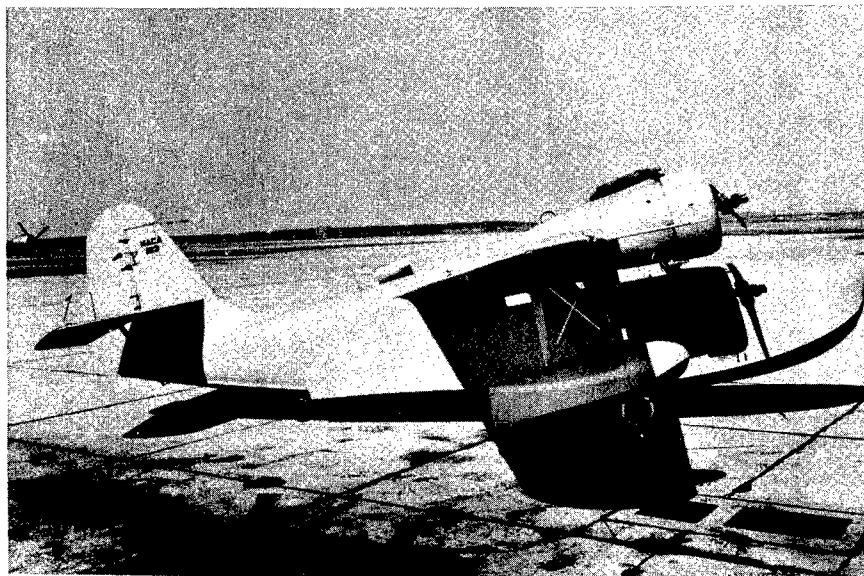


Figure 3.— Airspeed tube on airplane C.

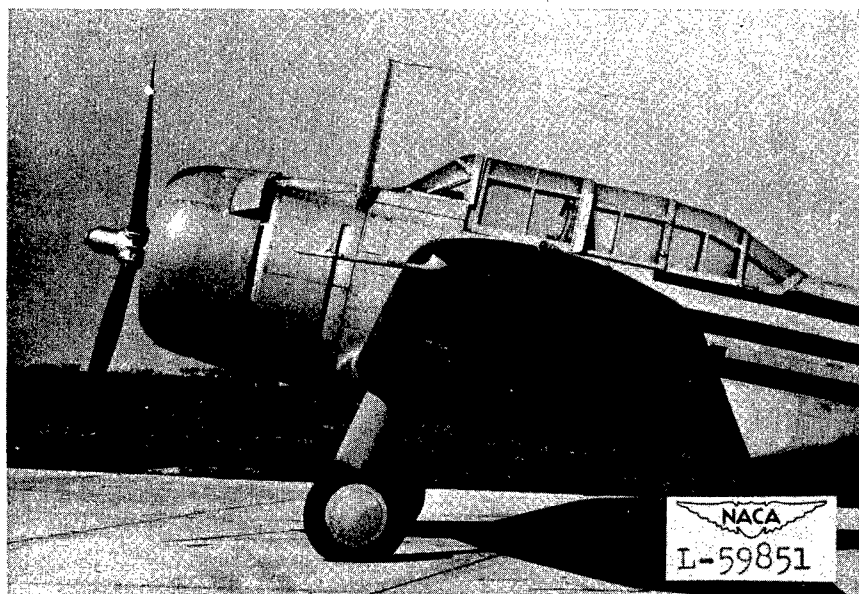


Figure 4.— Airspeed tube on airplane D.

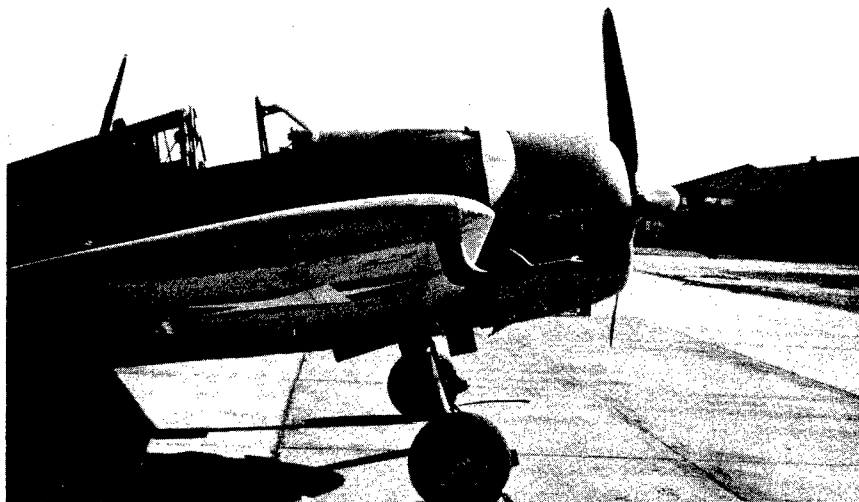


Figure 5.- Airspeed tube on airplane E.

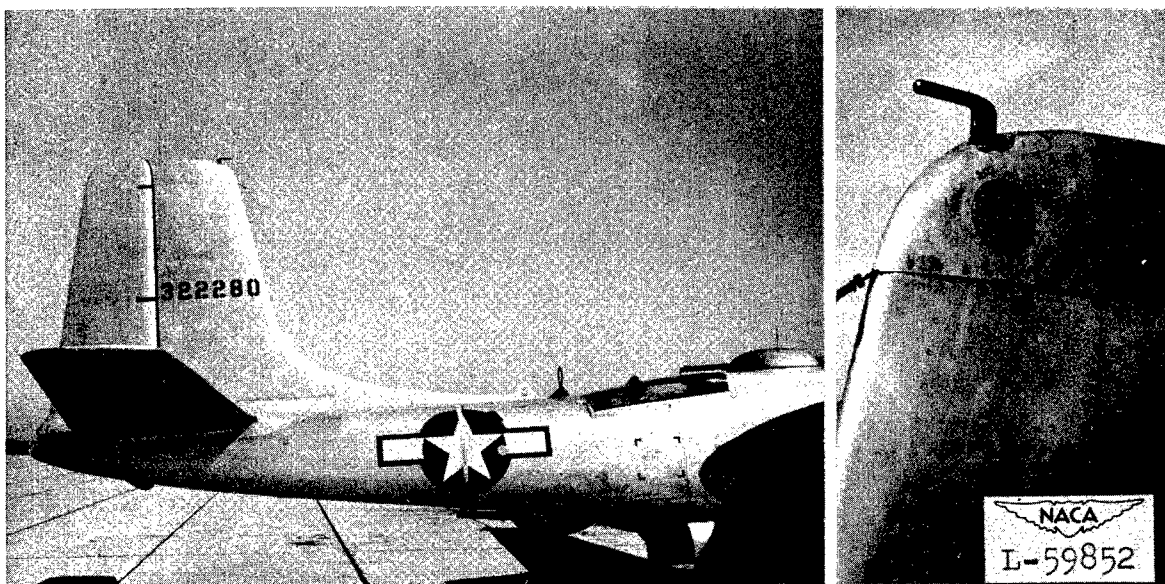


Figure 6.- Airspeed tube on airplane F.

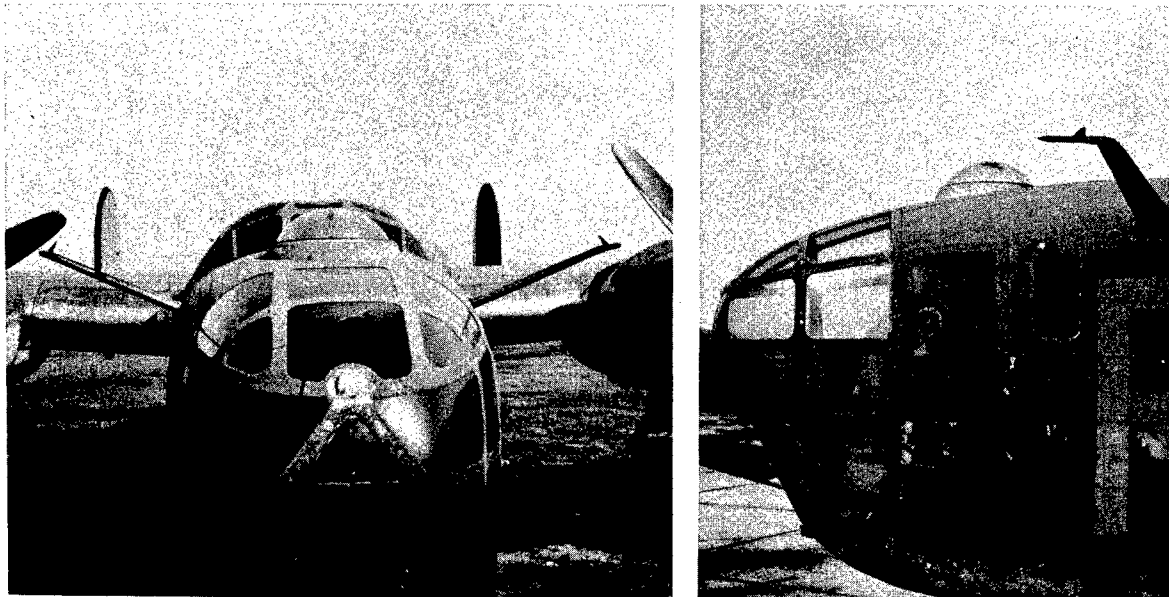


Figure 7.- Airspeed tubes on airplane G.

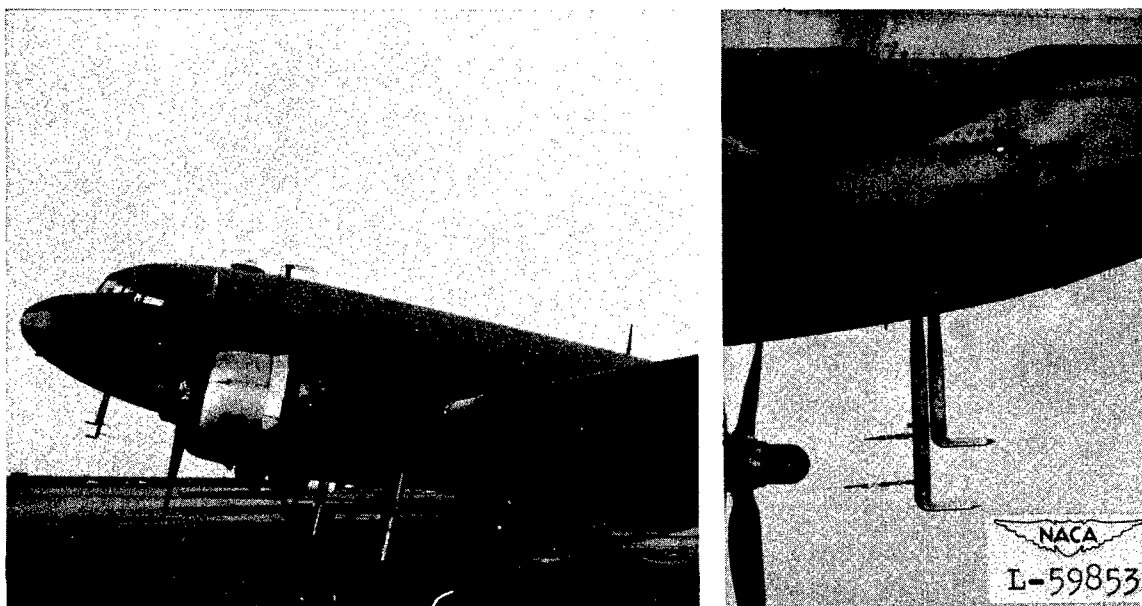


Figure 8.- Airspeed tubes on airplane H.



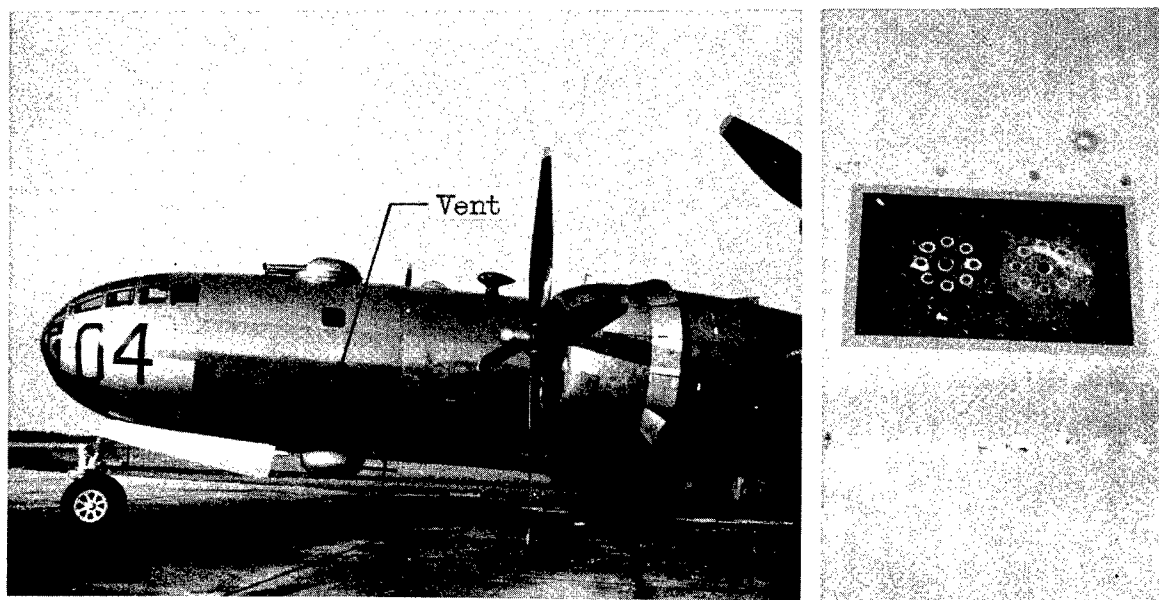


Figure 9.- Fuselage static-pressure vents on airplane I.

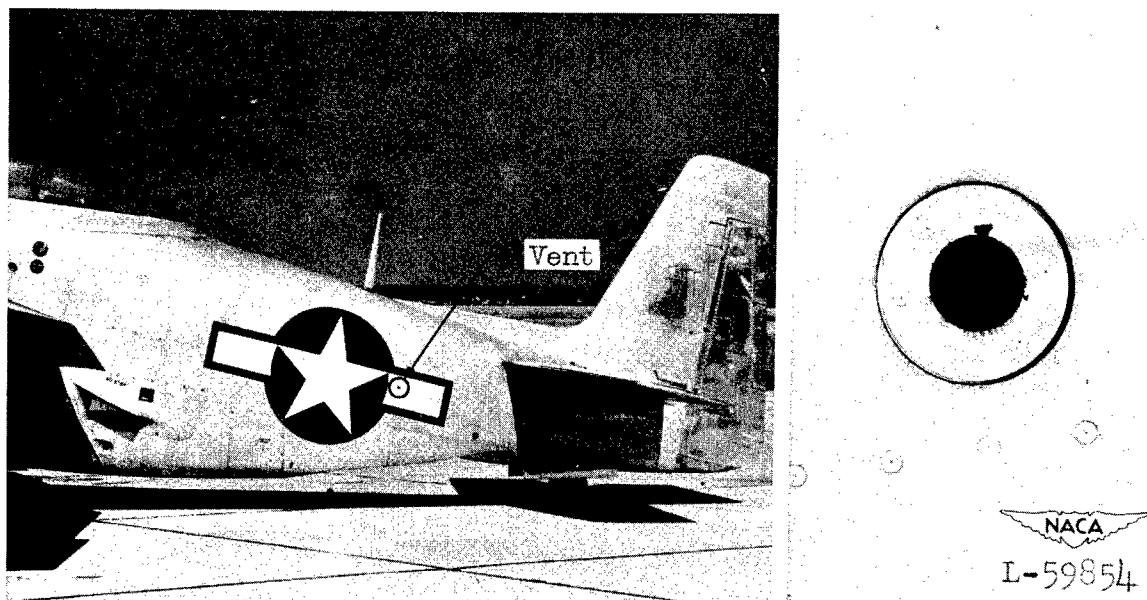


Figure 10.- Fuselage static-pressure vents on airplane J.

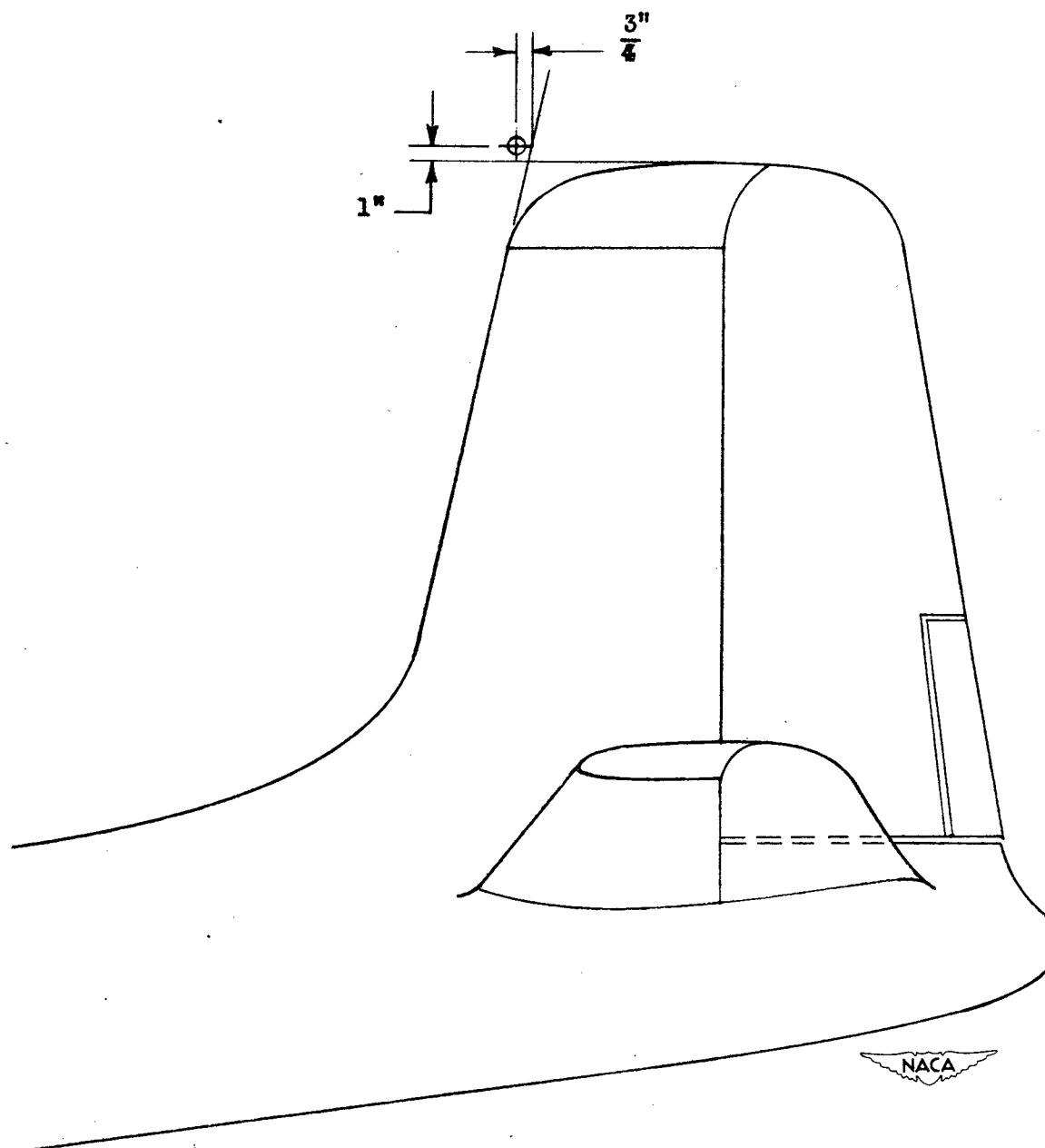


Figure 11.— Location of static-pressure orifices of pitot-static tube on airplane F. Pitot-static tube, Pioneer type 3218.

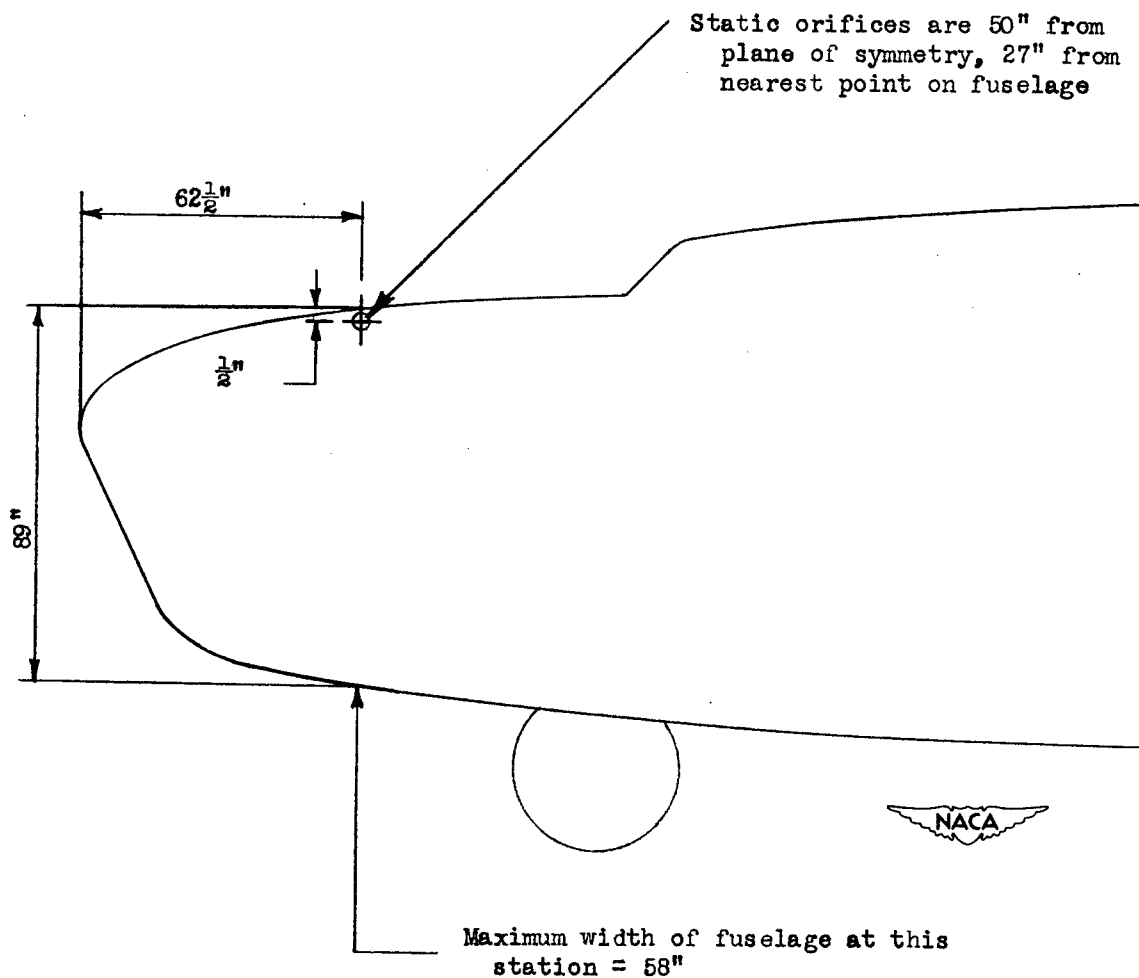


Figure 12.- Location of static-pressure orifices of the two pitot-static tubes on airplane G. Pitot-static tubes, Kollsman type 369.

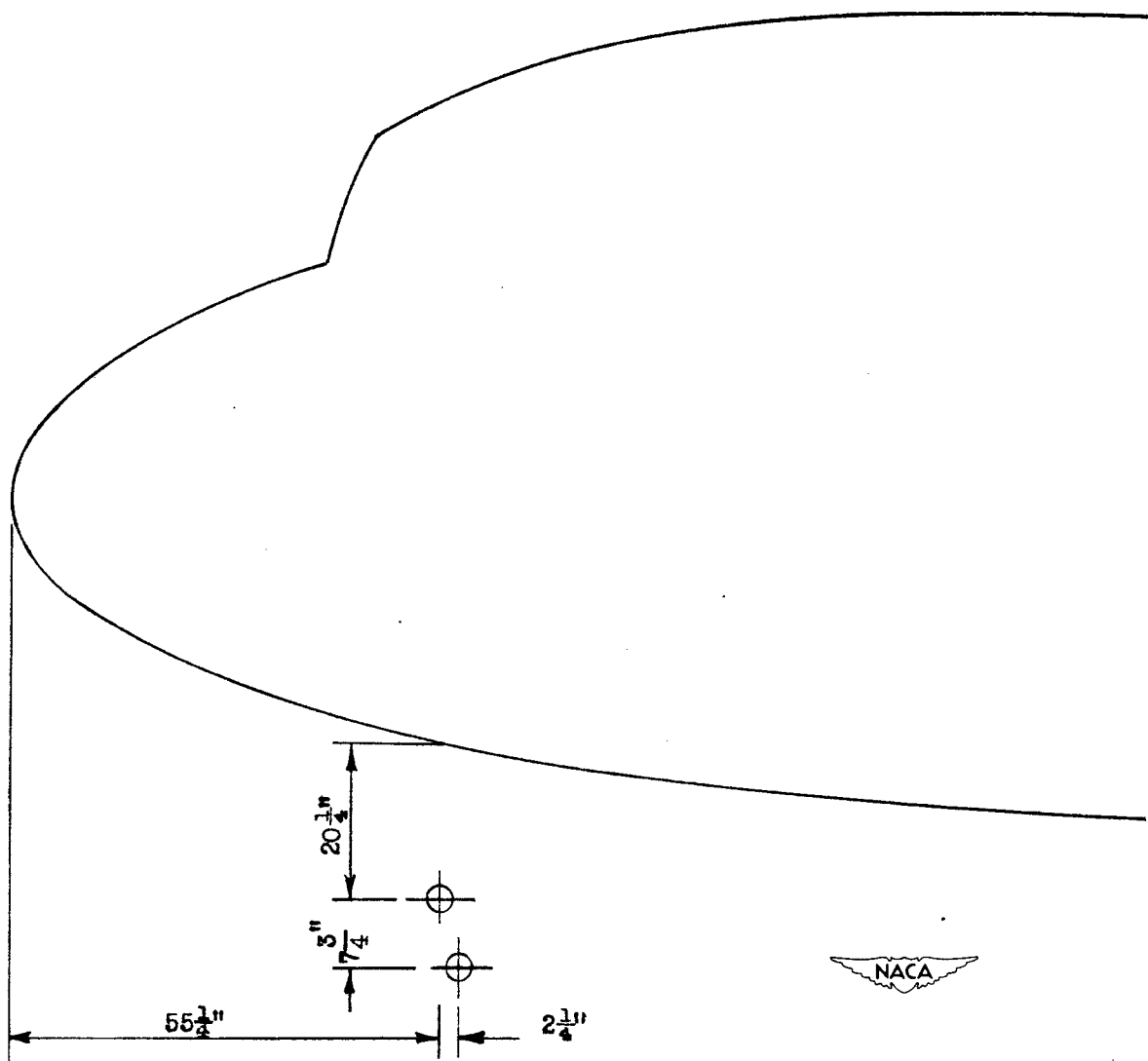


Figure 13.— Location of static-pressure orifices of the two pitot-static tubes on airplane H. Pitot-static tubes, Kollsman type 373.

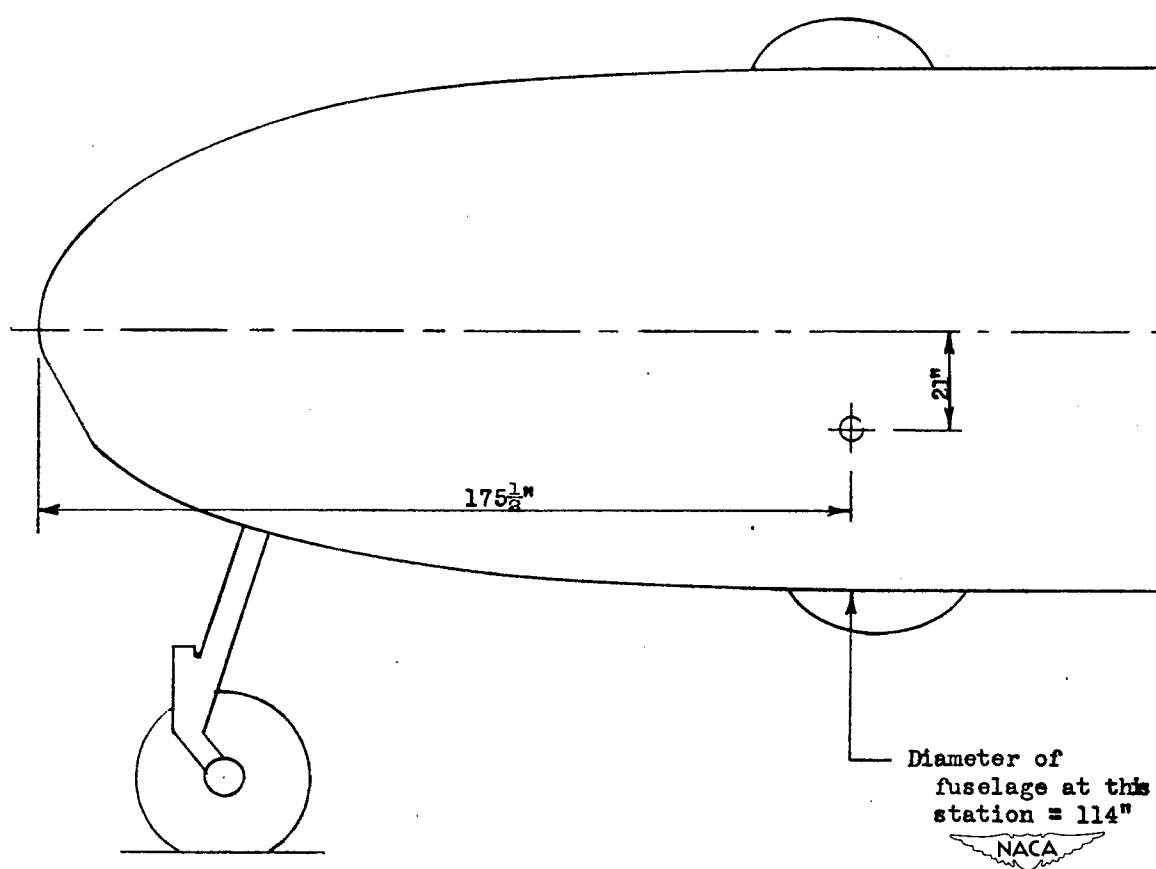


Figure 14.- Location of fuselage static-pressure vents on airplane I.

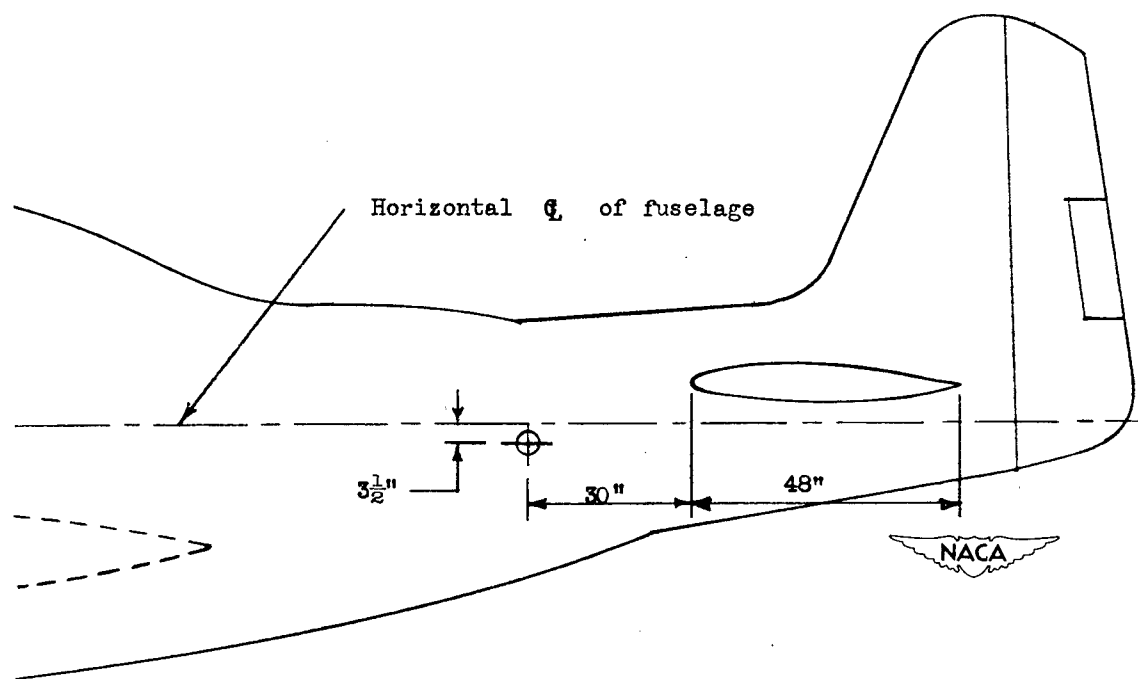


Figure 15.- Location of fuselage static-pressure vents on airplane J.

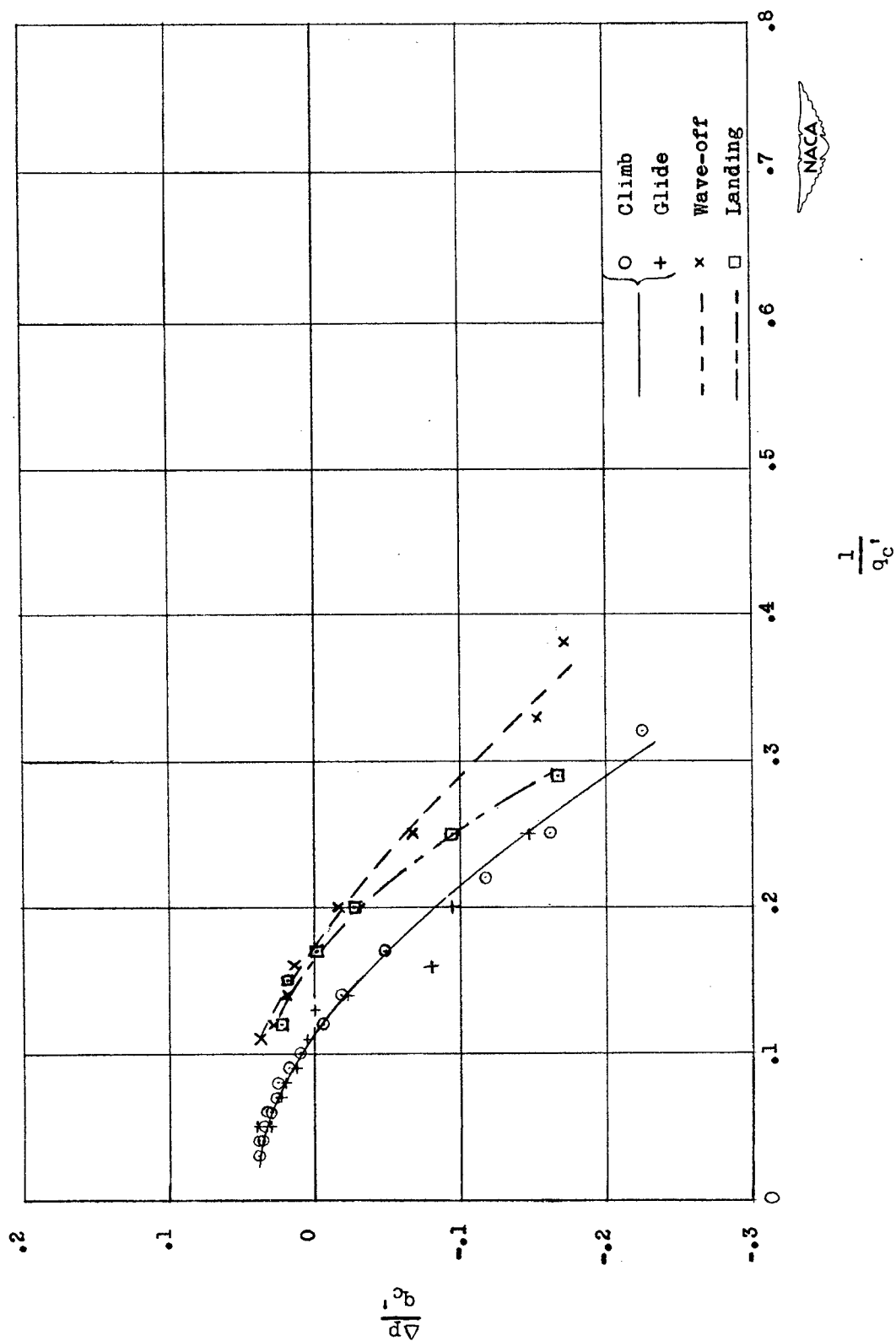


Figure 16.— Calibration of the position error of the service static installation on airplane A.

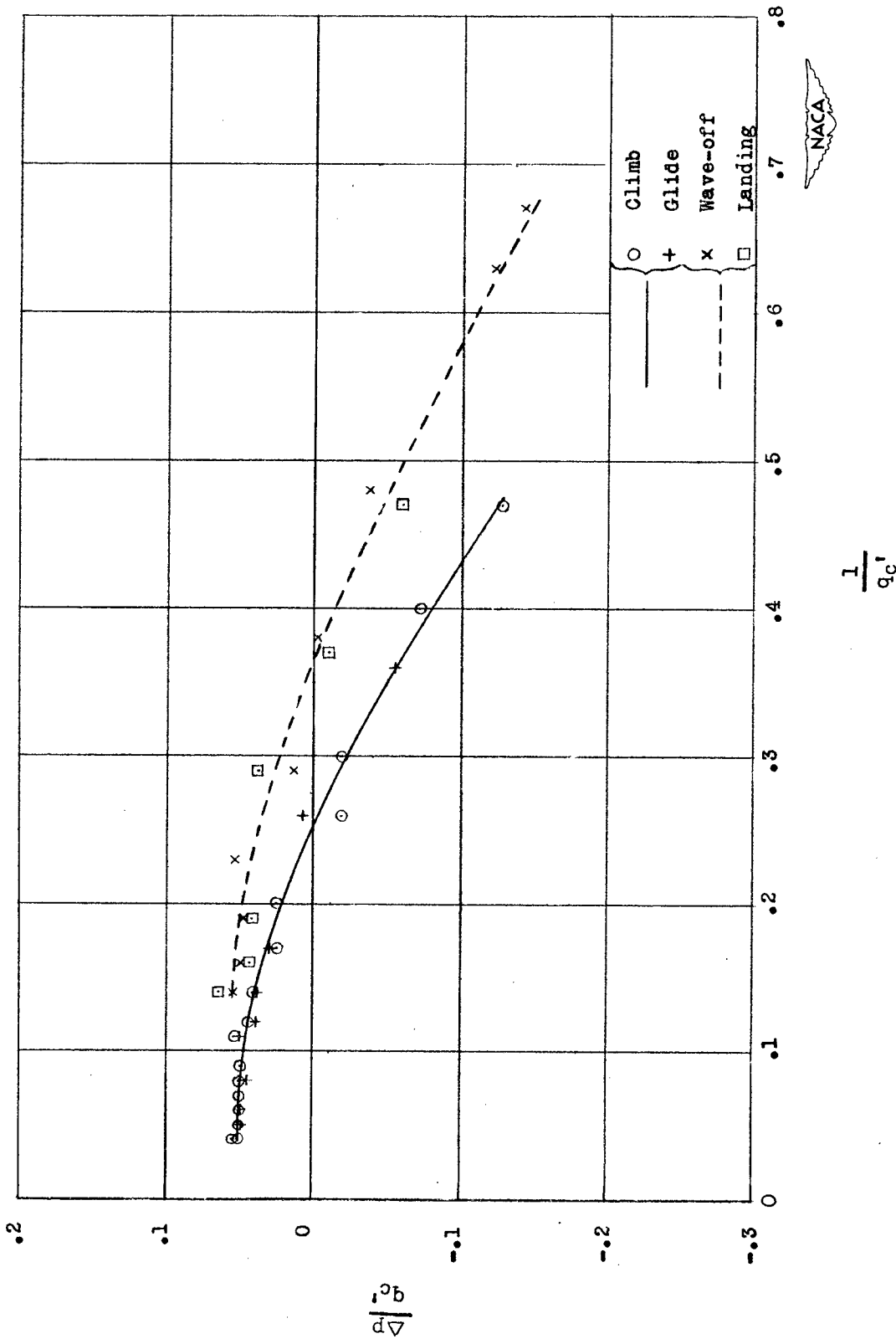


Figure 17.- Calibration of the position error of the service static installation on airplane B.



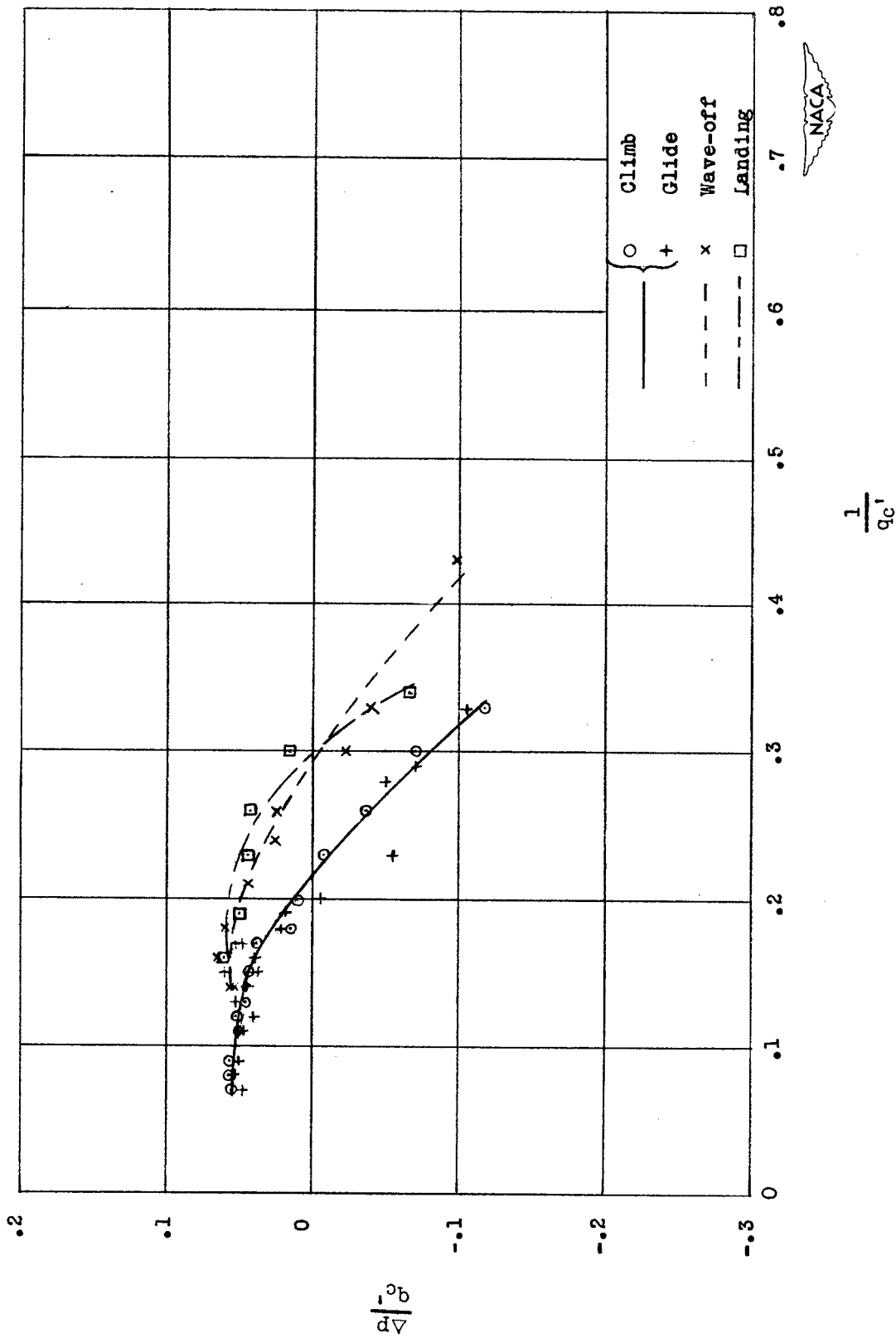


Figure 18.— Calibration of the position error of the service static installation on airplane C.

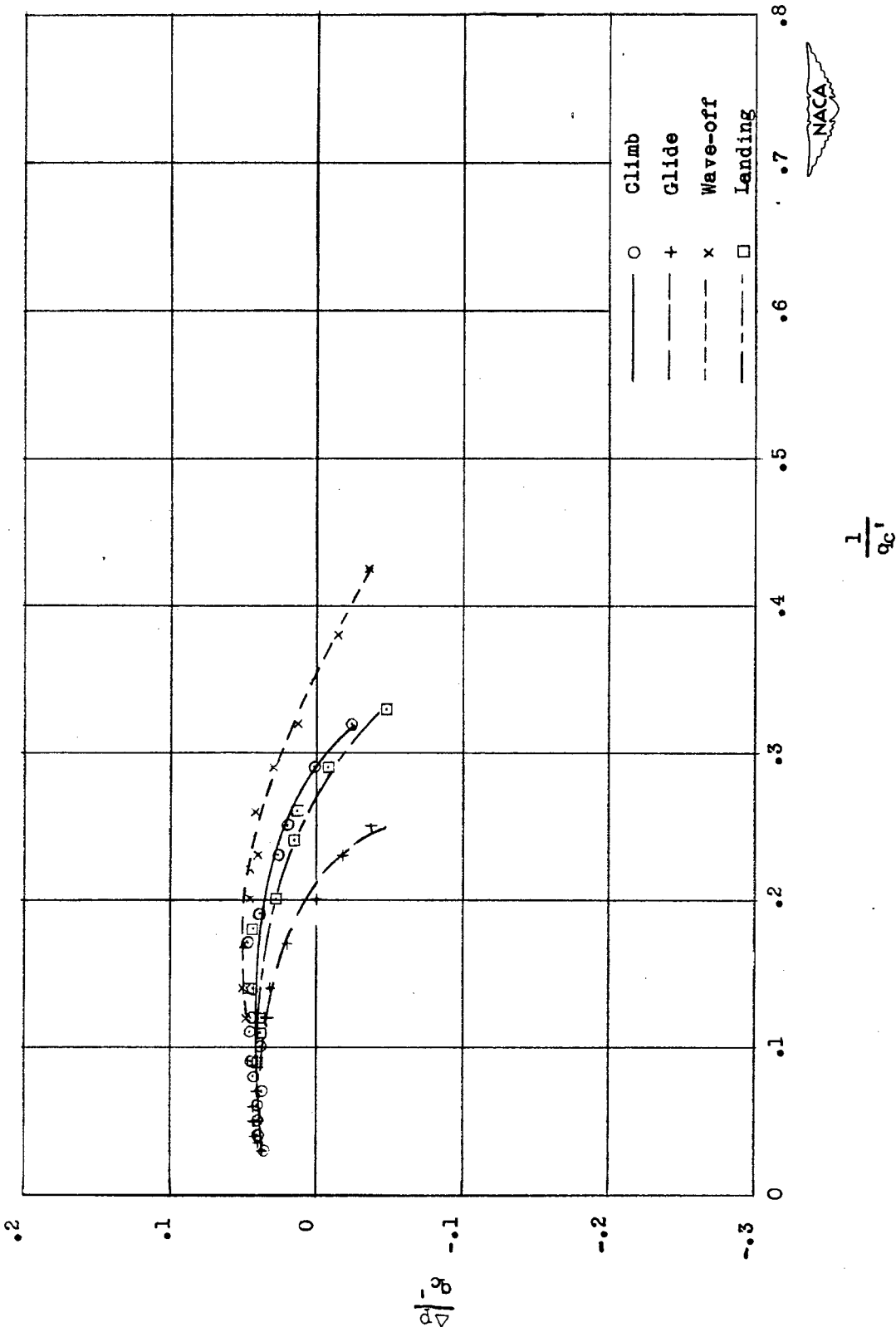


Figure 19.- Calibration of the position error of the service static installation on airplane D.

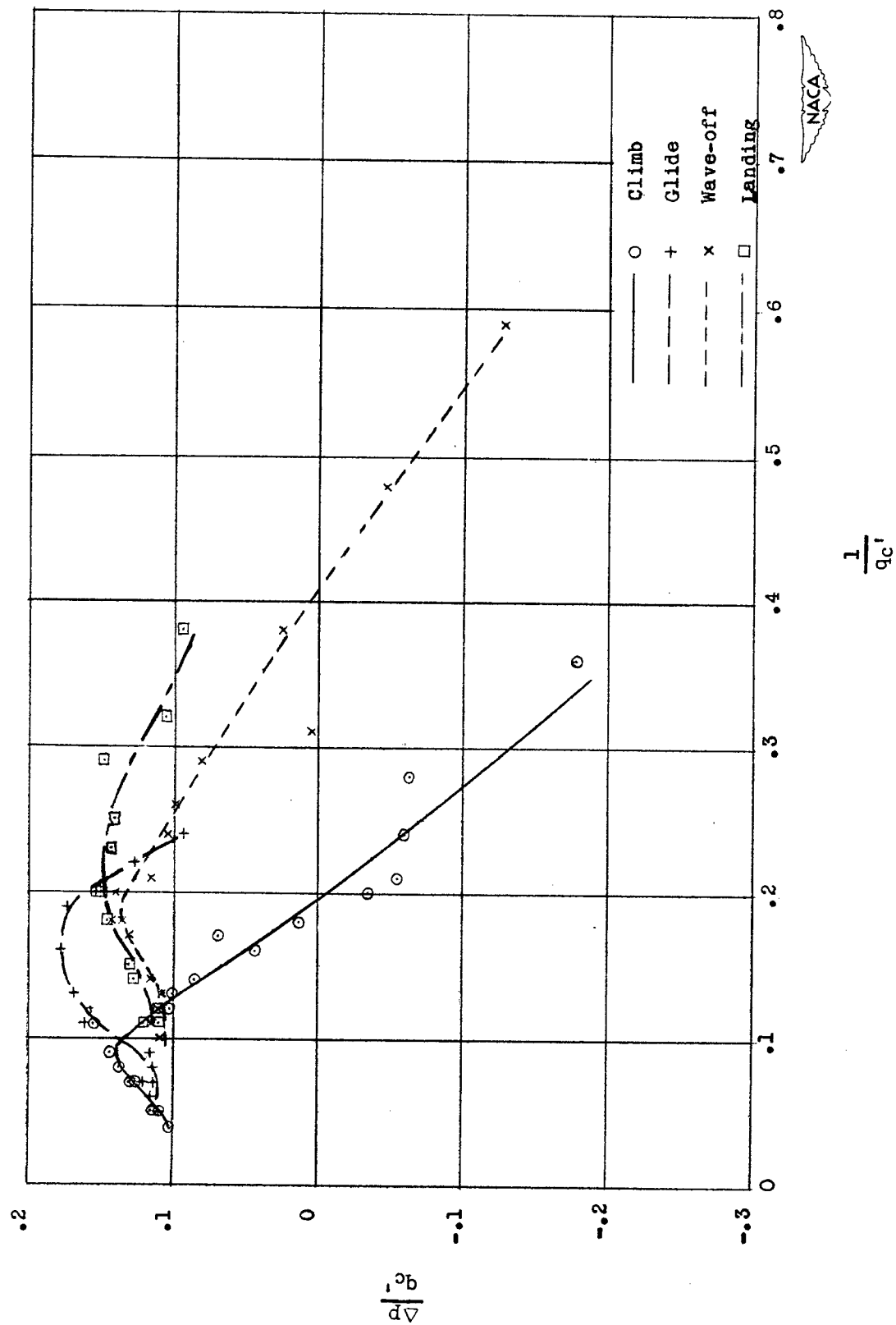
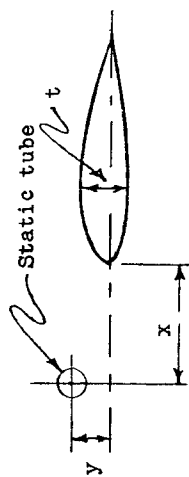


Figure 20.— Calibration of the position error of the service static installation on airplane E.



The sign of  $y$  is positive when the orifices are located above the extension of the chord line

	Airplane	$y$ , in.
○	A	13.0
□	B	-5
◇	C	-2.0
△	D	-5.5
▽	E	-6.5
○	Reference 3	0
---	Pairing of flight data	

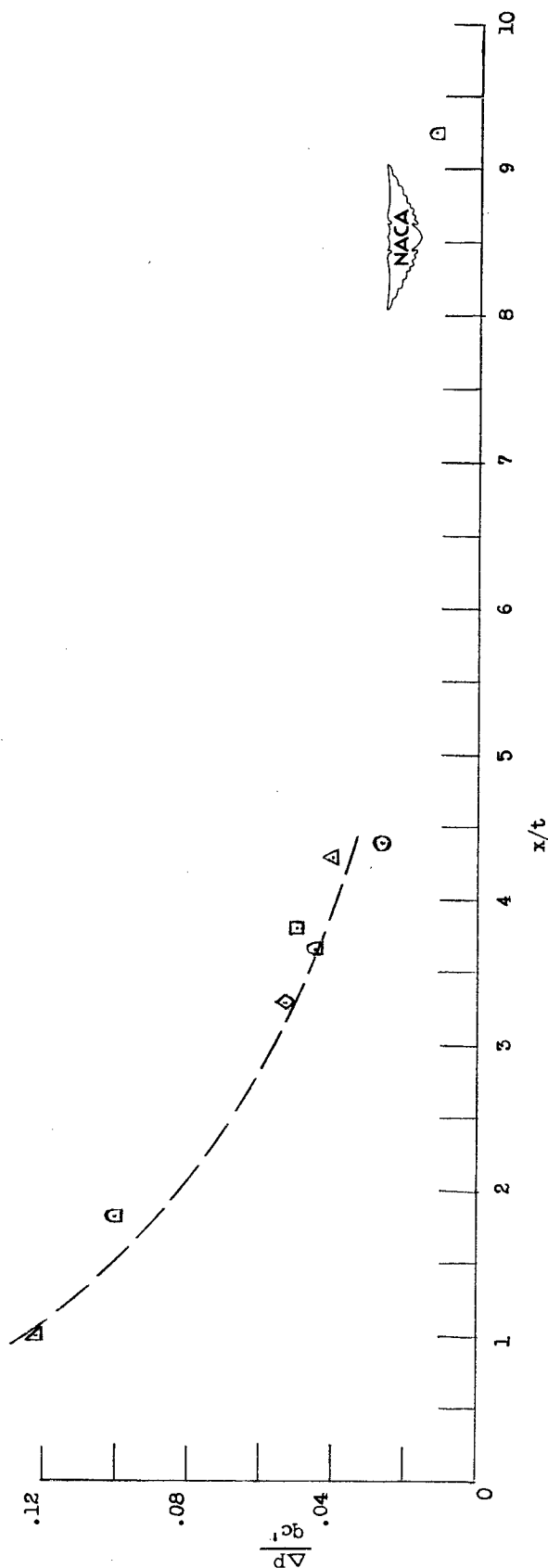


Figure 21.— Static-pressure error as a function of the position of static orifices ahead of a wing (based on the position errors of five wing installations at a lift coefficient of 0.4). (Data from reference 3 for Mach number of 0.4 and angle of attack of  $0^\circ$ .)

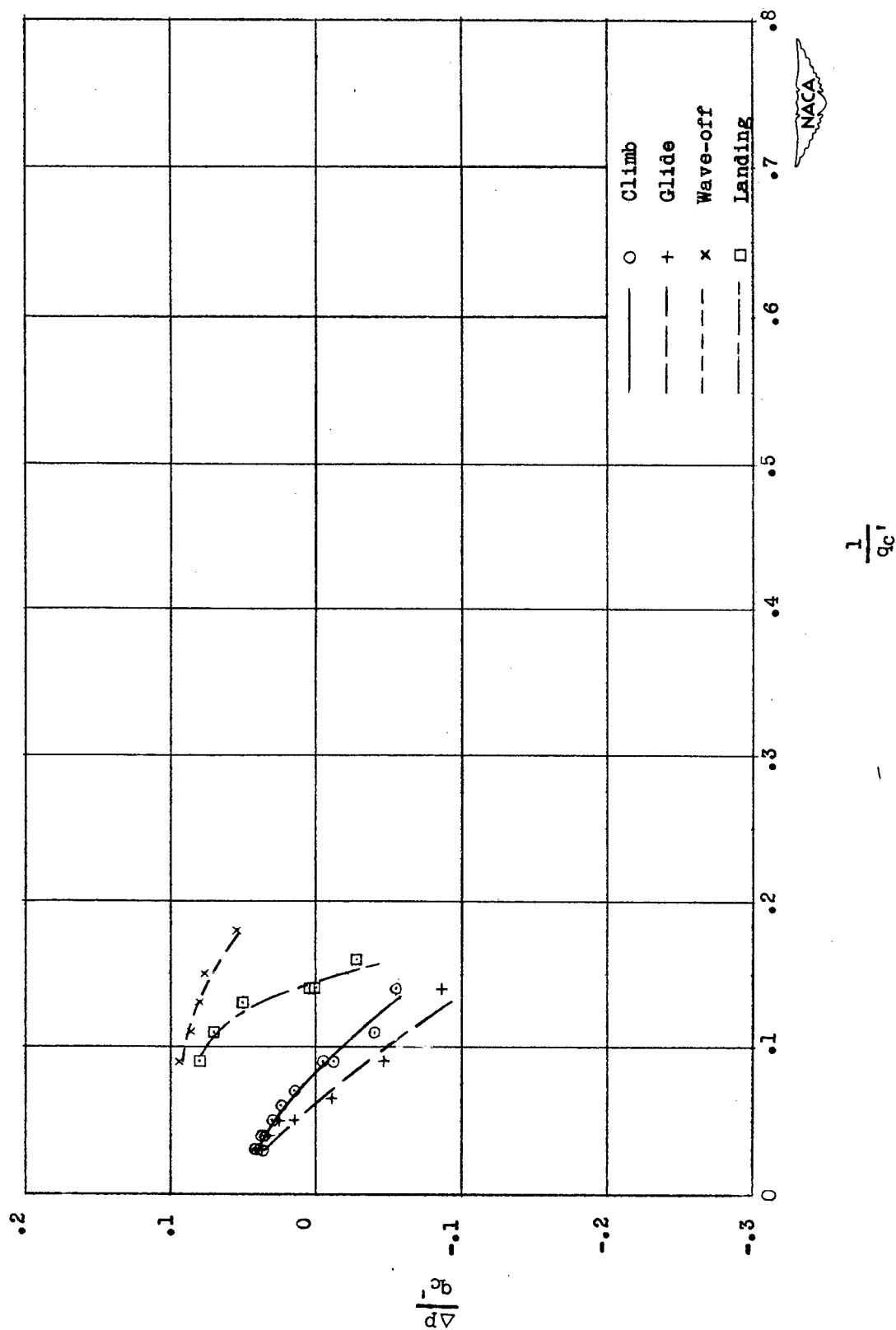


Figure 22.— Calibration of the position error of the service static installation on airplane F.

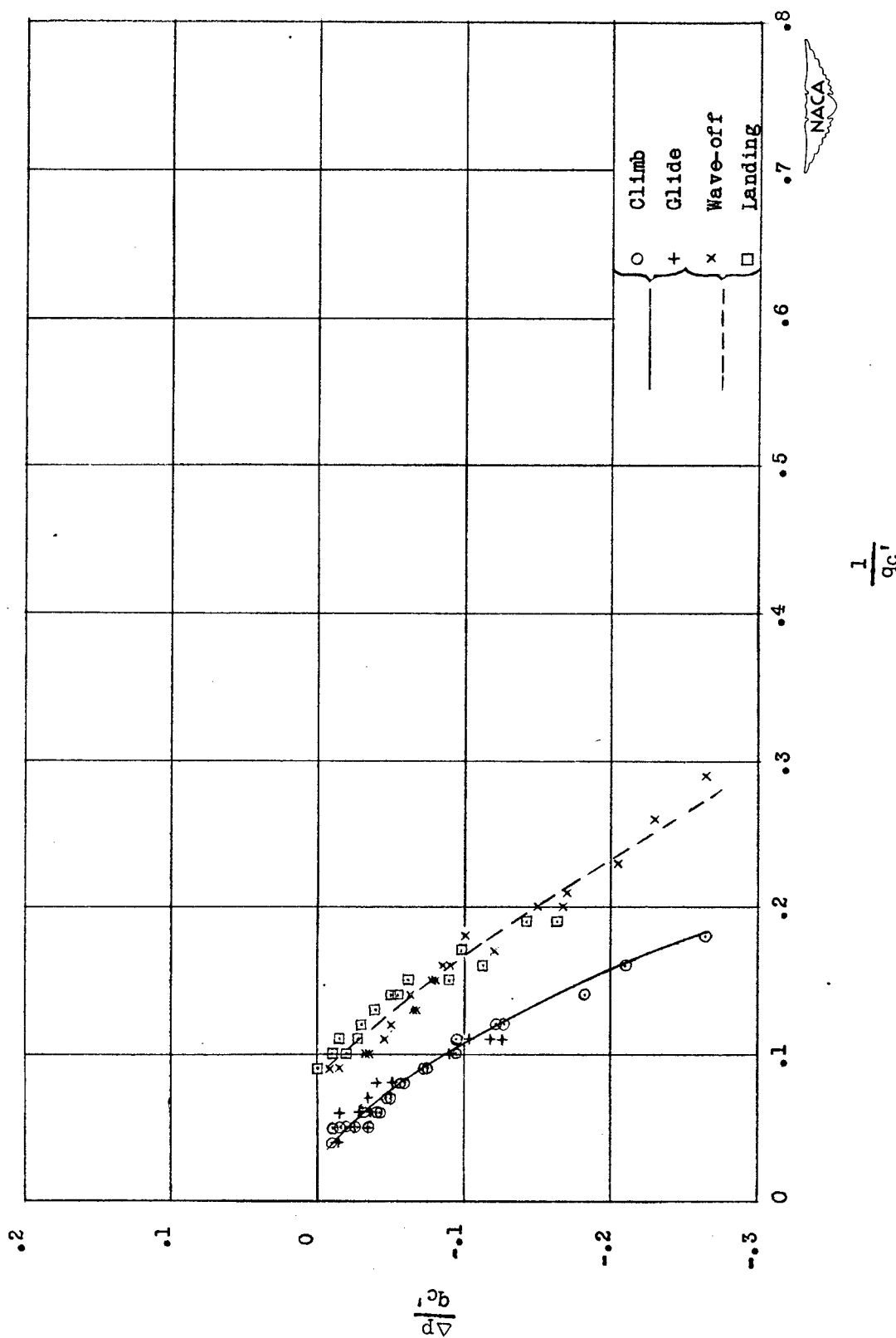


Figure 23.- Calibration of the position error of the service static installation on airplane G.

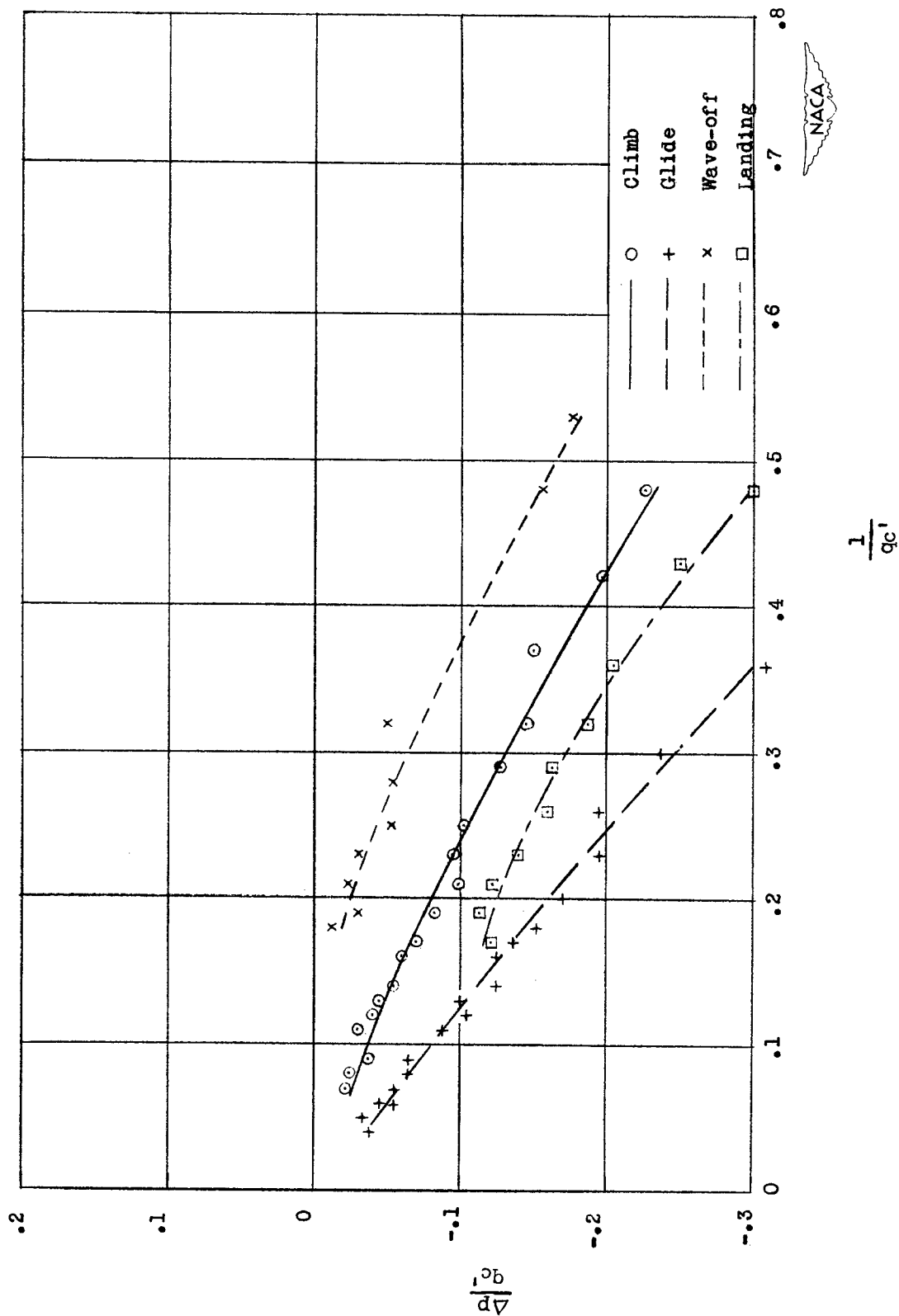


Figure 24.— Calibration of the position error of the service static installation on airplane H.

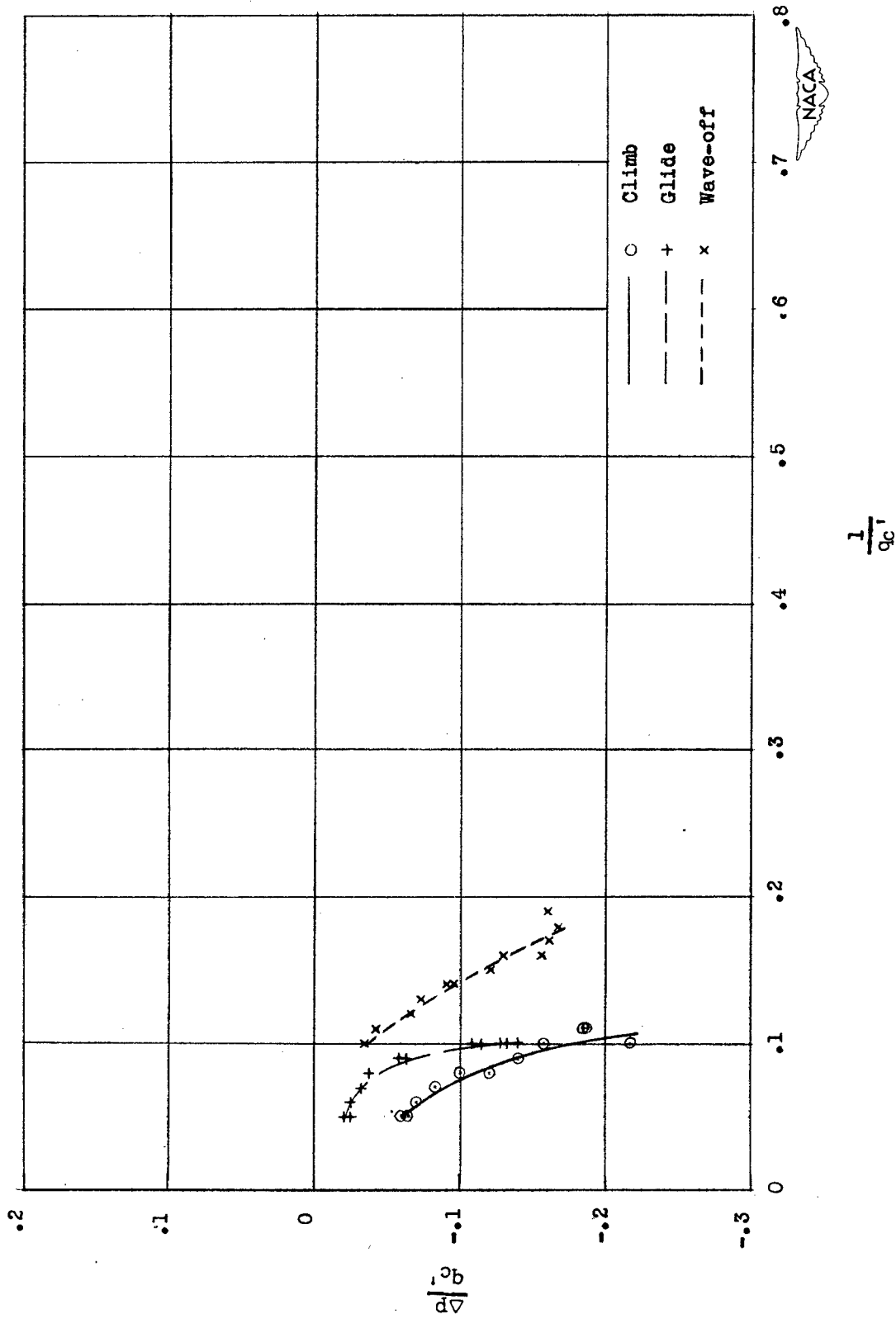


Figure 25.— Calibration of the position error of the service static installation on airplane I.



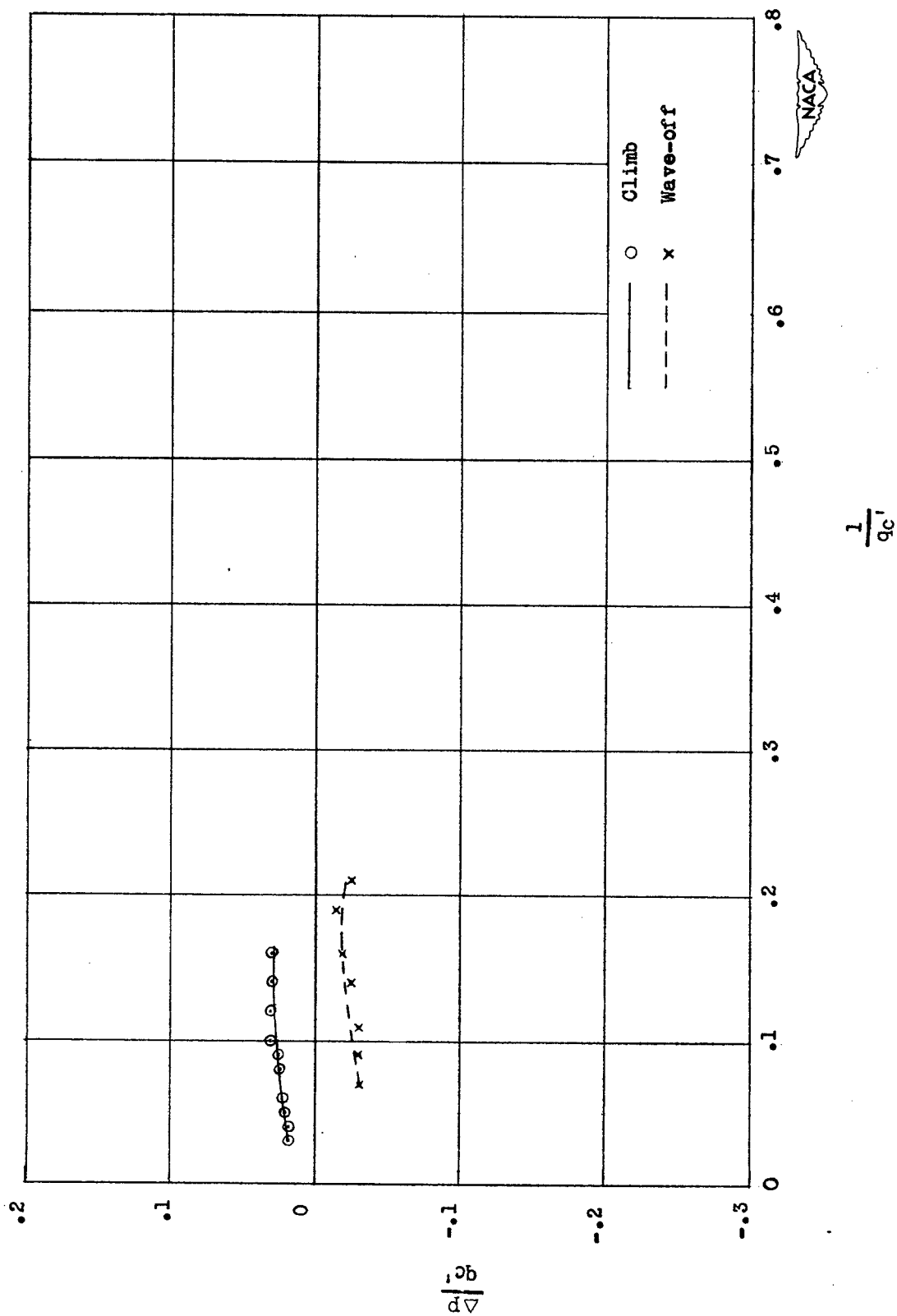


Figure 26.— Calibration of the position error of the service static installation on airplane J.

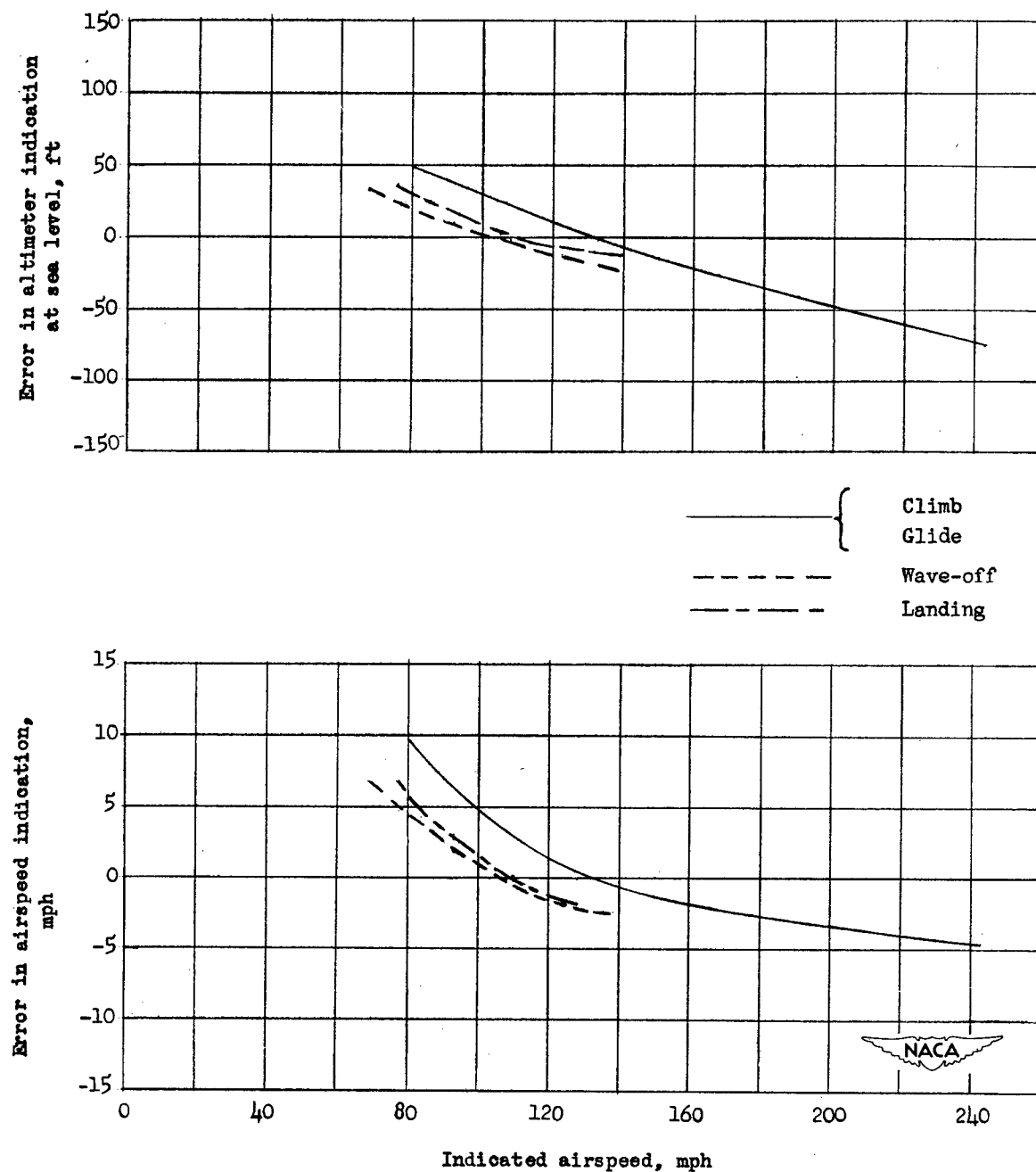


Figure 27.— Errors in airspeed and altimeter indication due to position error of static tube. Airplane A.

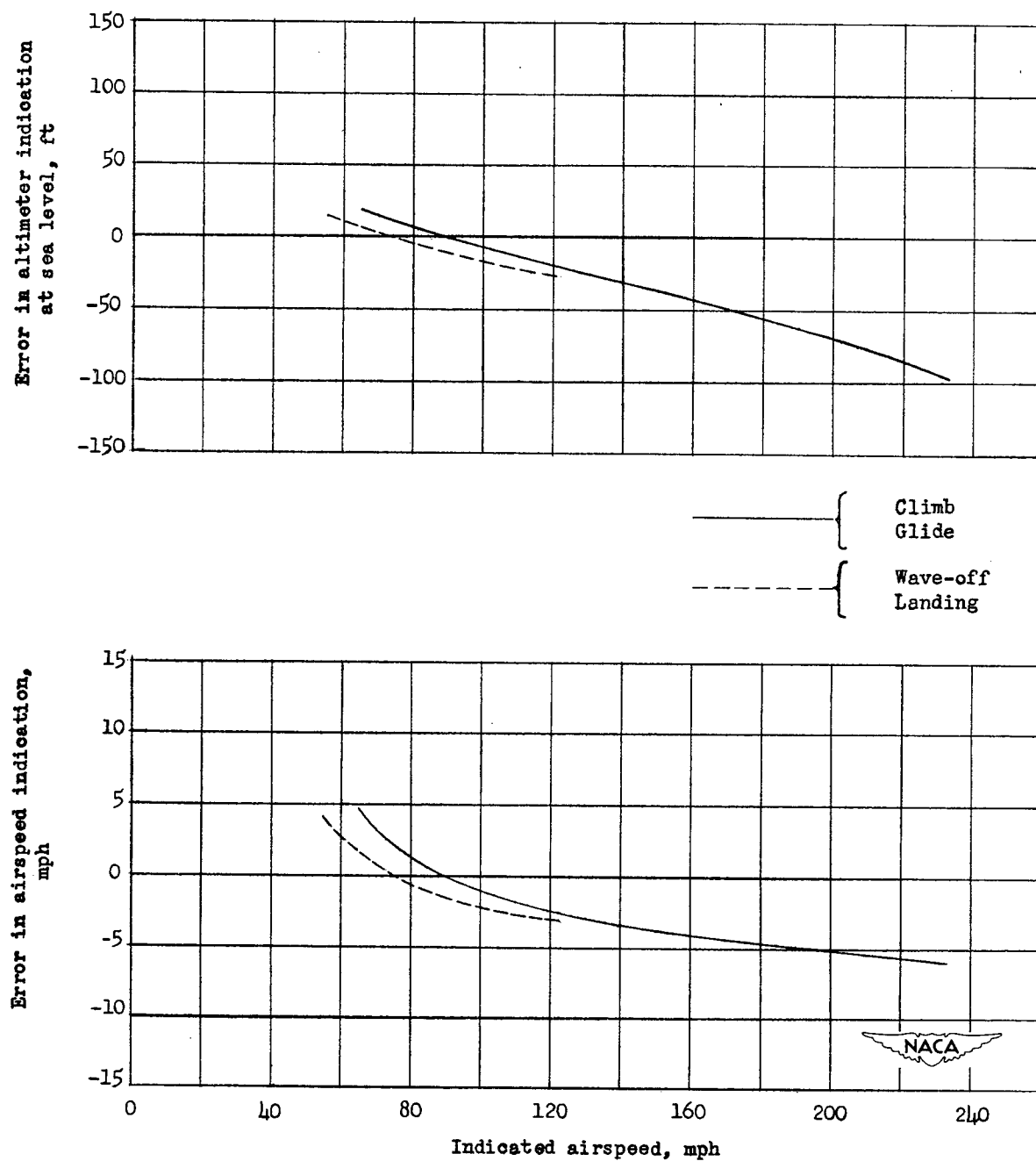


Figure 28.- Errors in airspeed and altimeter indication due to position error of static tube. Airplane B.

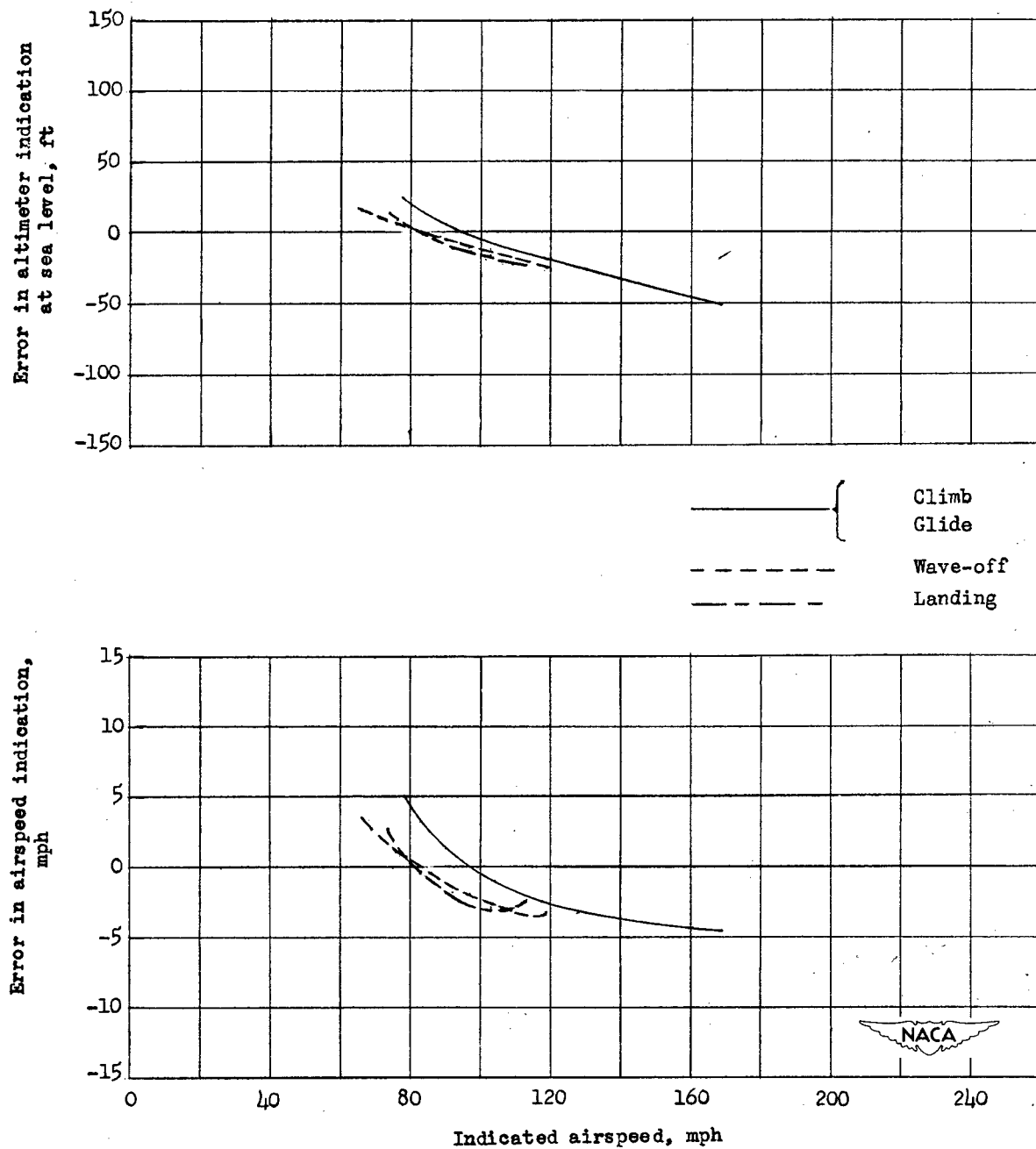


Figure 29.— Errors in airspeed and altimeter indication due to position error of static tube. Airplane C.

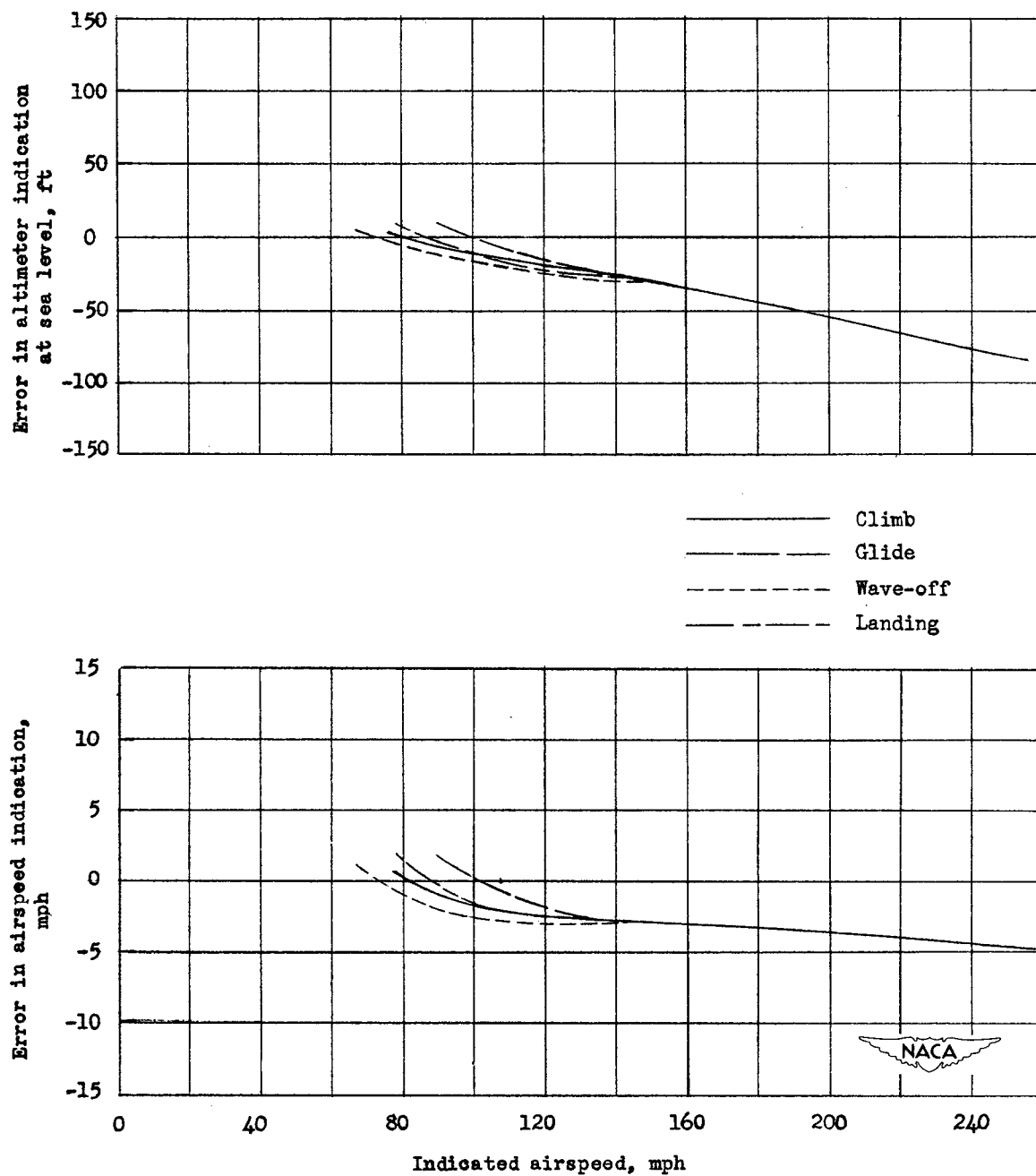


Figure 30.— Errors in airspeed and altimeter indication due to position error of static tube. Airplane D.

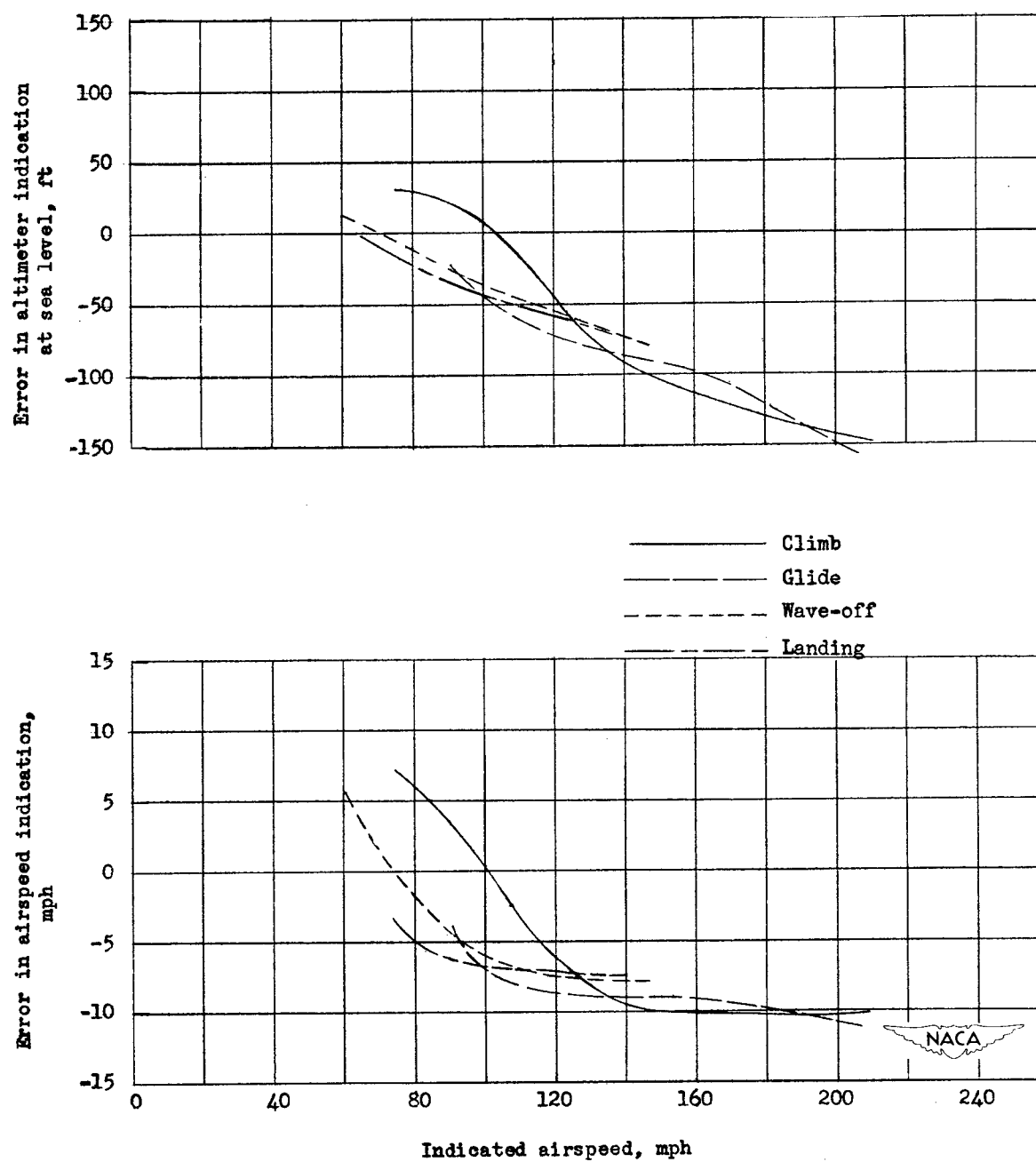


Figure 31.— Errors in airspeed and altimeter indication due to position error of static tube. Airplane E.

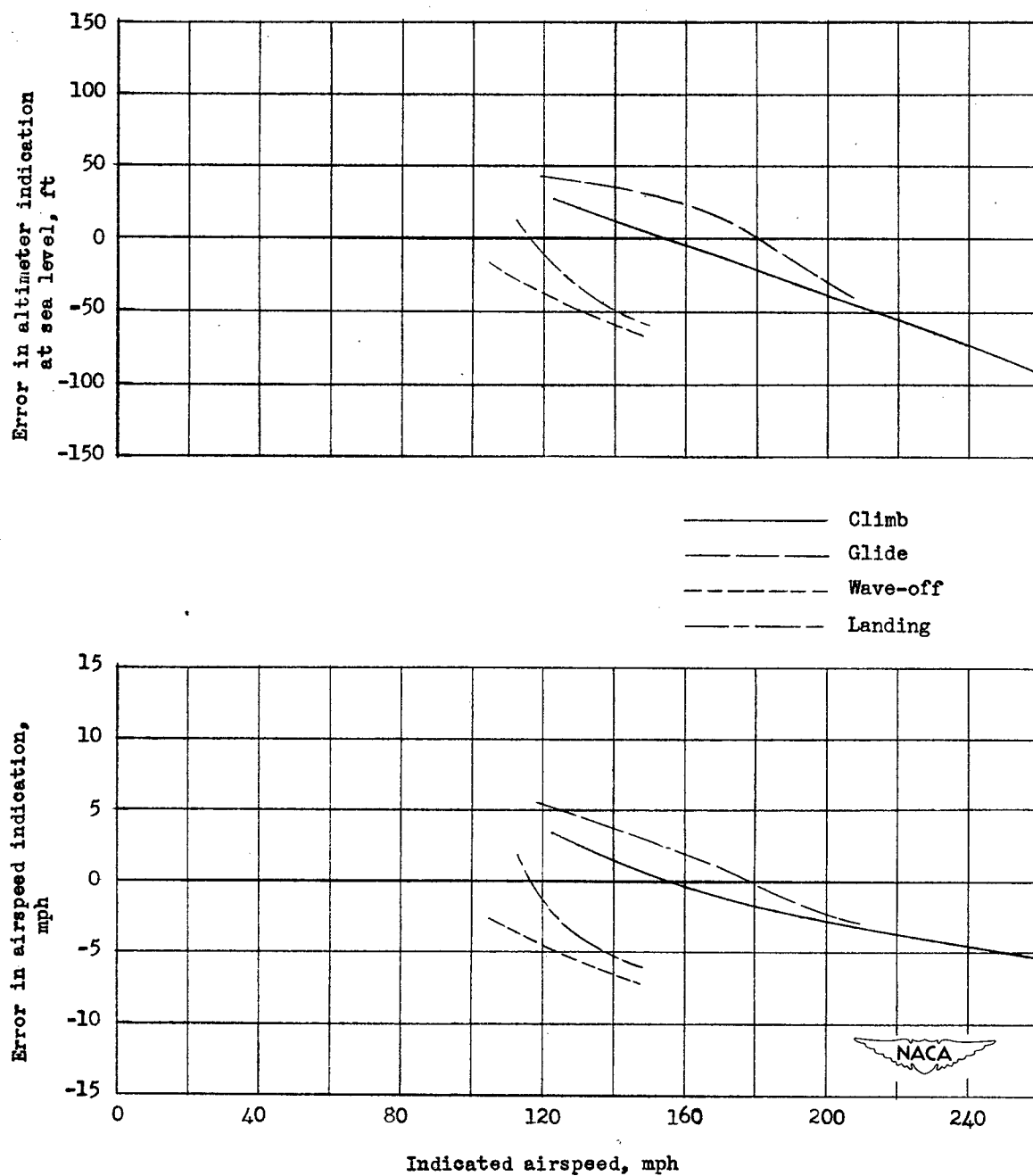


Figure 32.— Errors in airspeed and altimeter indication due to position error of static tube. Airplane F.

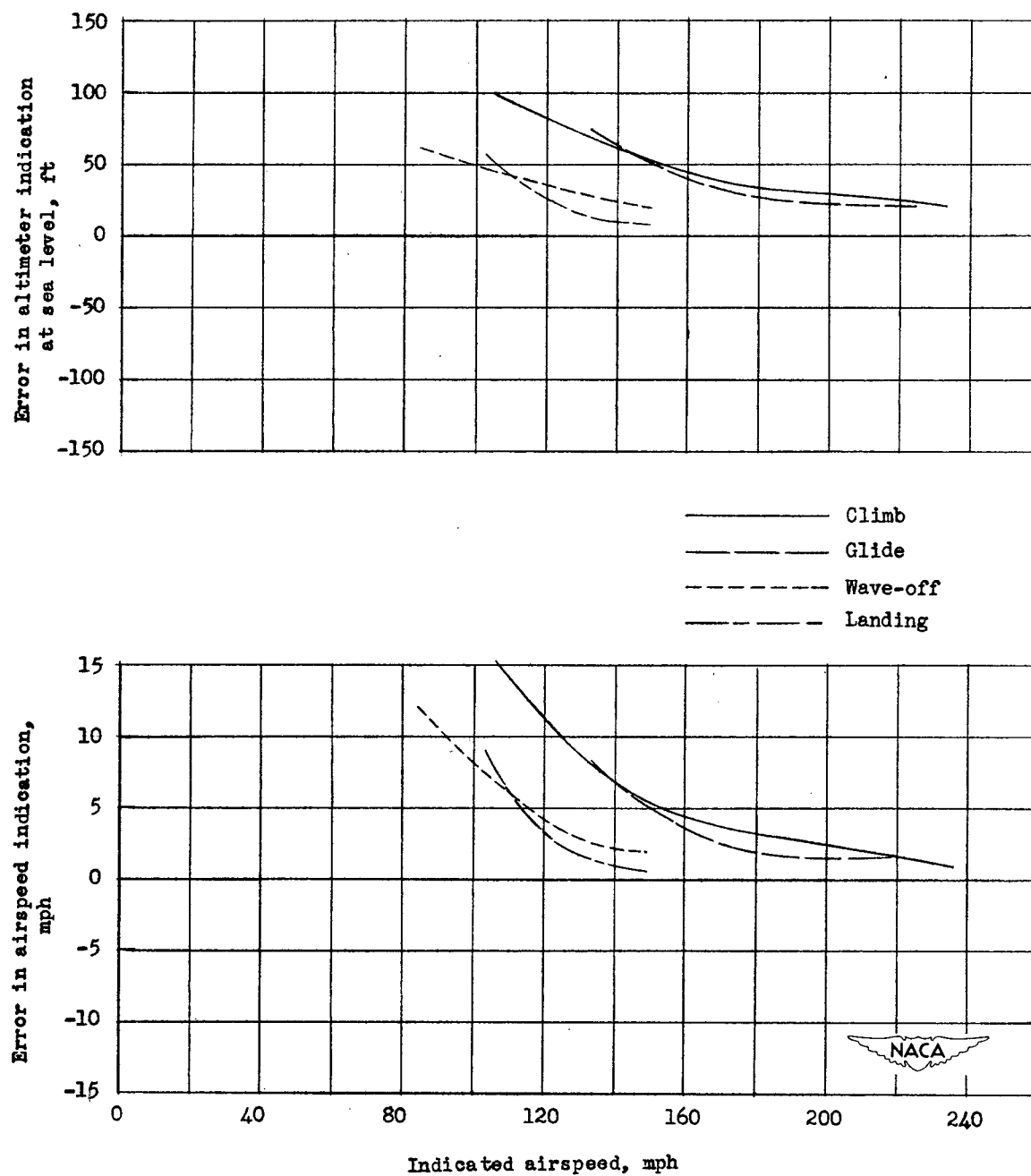


Figure 33.— Errors in airspeed and altimeter indication due to position error of static tube. Airplane G.



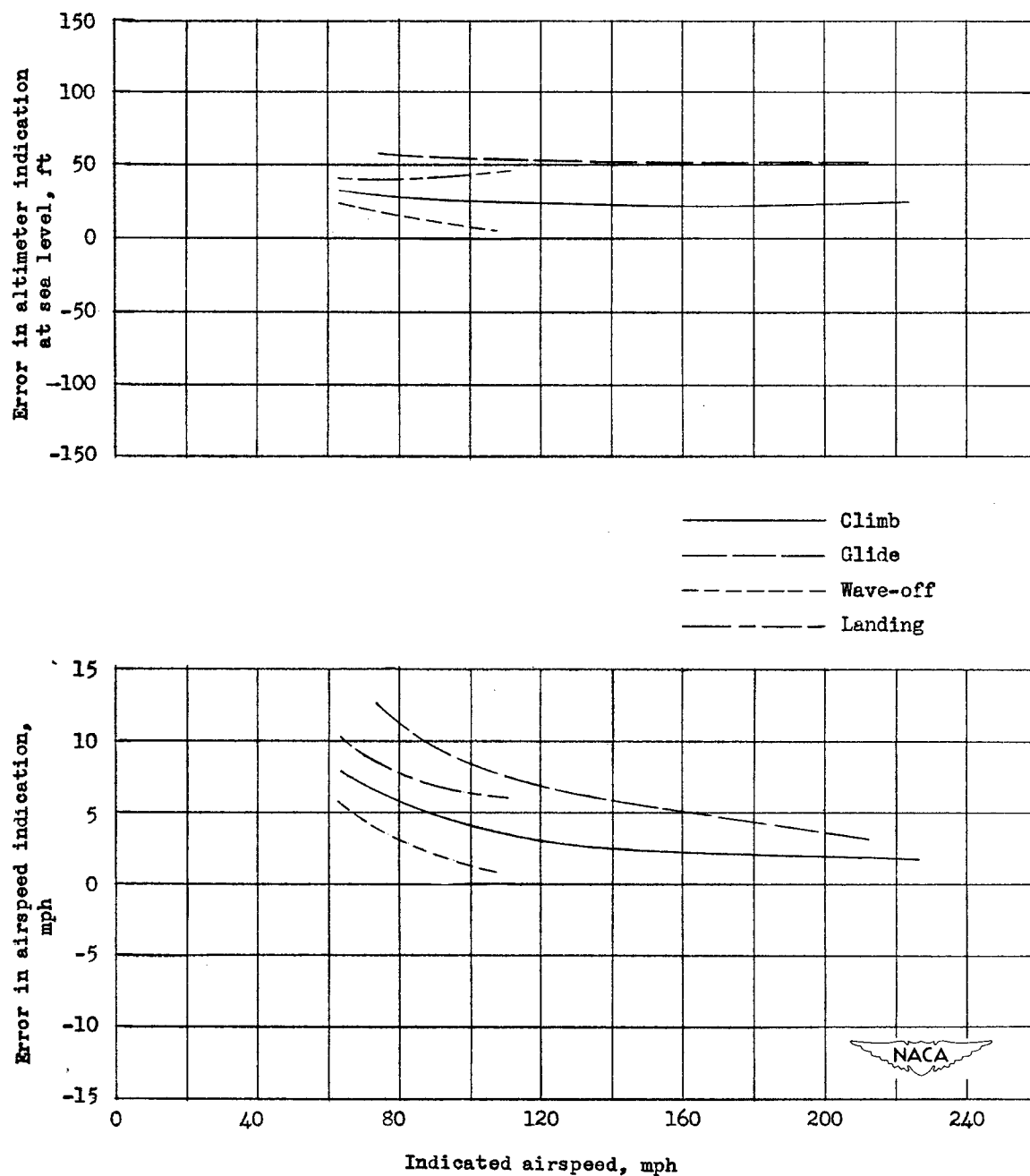


Figure 34.— Errors in airspeed and altimeter indication due to position error of static tube. Airplane H.

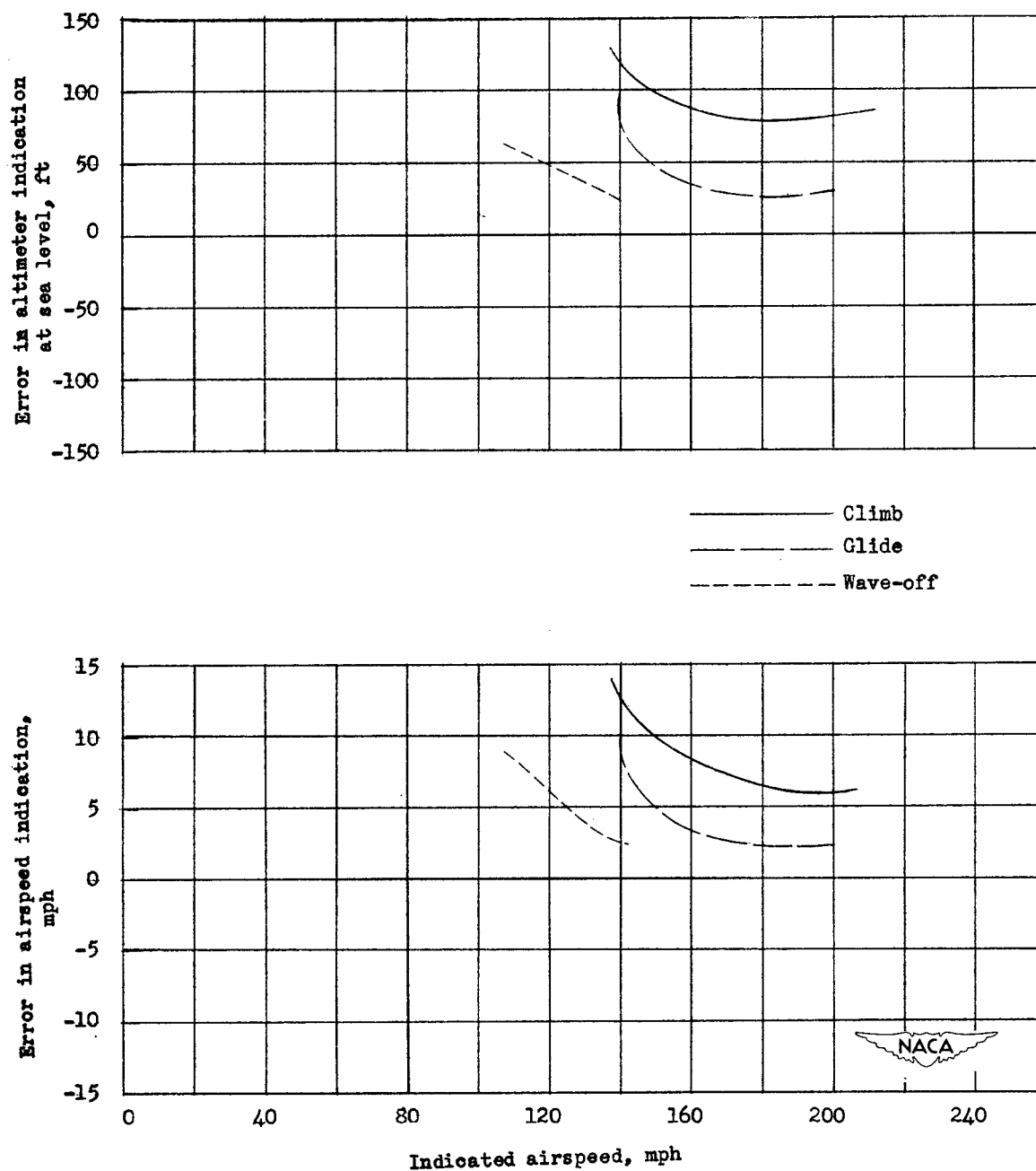


Figure 35.— Errors in airspeed and altimeter indication due to position error of static tube. Airplane I.

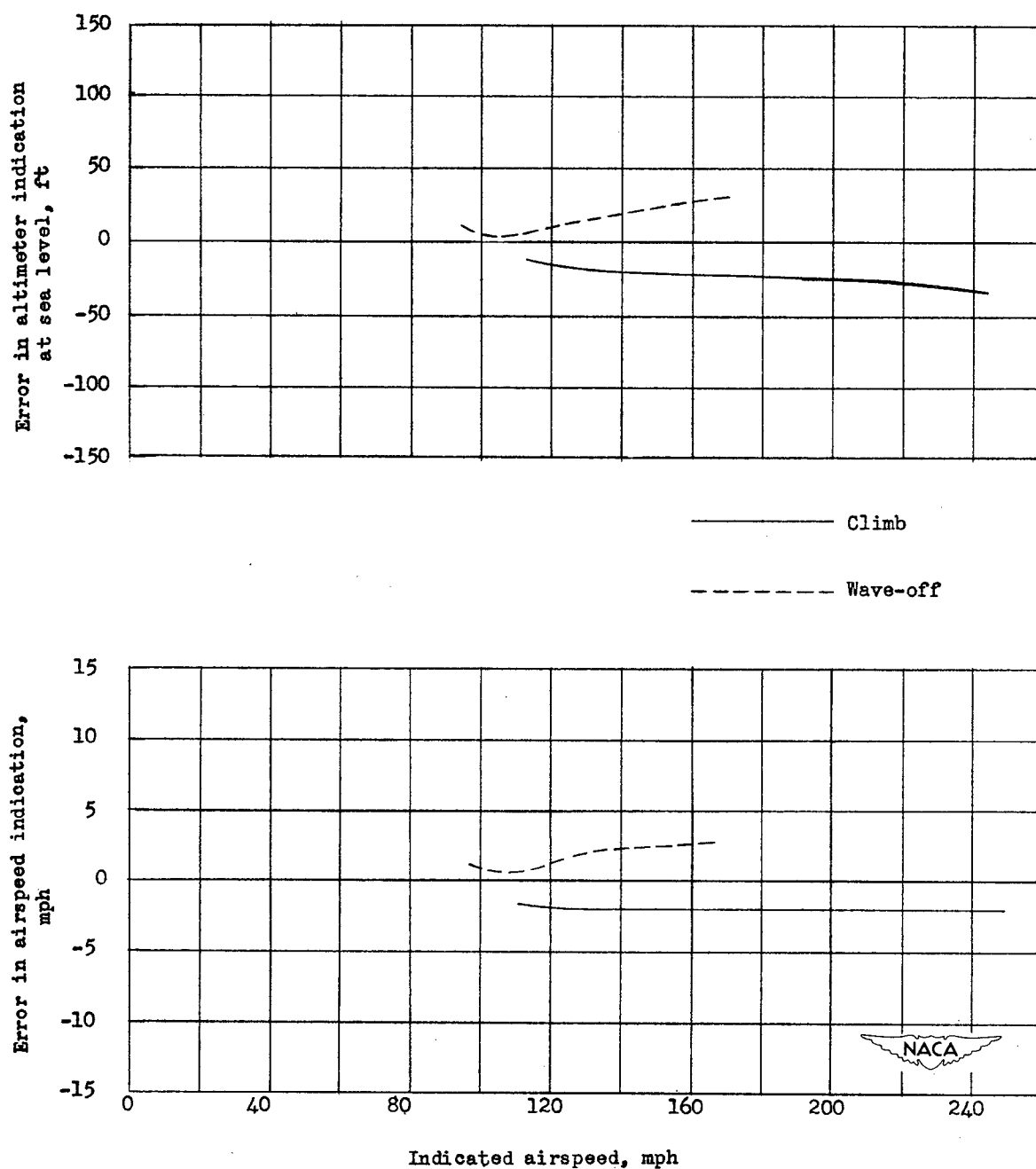


Figure 36.— Errors in airspeed and altimeter indication due to position error of static tube. Airplane J.

Navigation

7.2



Position Errors of the Service Airspeed Installations of 10 Airplanes.

By William Gracey

NACA TN 1892  
June 1949

(Abstract on Reverse Side)

Research Techniques - Correction

9.2.1



Position Errors of the Service Airspeed Installations of 10 Airplanes.

By William Gracey

NACA TN 1892  
June 1949

(Abstract on Reverse Side)

Gracey, William



Position Errors of the Service Airspeed Installations of 10 Airplanes.

By William Gracey

NACA TN 1892  
June 1949

(Abstract on Reverse Side)

### Abstract

The "position" errors of the static systems of 10 service airspeed installations including static-pressure vents on the nose and rear section of the fuselage and pitot-static tubes mounted on the wing, the vertical tail, and the fuselage nose are presented. Tests were conducted at speeds between the stalling speed and 260 miles per hour for four flight conditions. Calibrations are analyzed to show variation of static-pressure error with position of static source, angle of attack, flap setting, and engine power.

### Abstract

The "position" errors of the static systems of 10 service airspeed installations including static-pressure vents on the nose and rear section of the fuselage and pitot-static tubes mounted on the wing, the vertical tail, and the fuselage nose are presented. Tests were conducted at speeds between the stalling speed and 260 miles per hour for four flight conditions. Calibrations are analyzed to show variation of static-pressure error with position of static source, angle of attack, flap setting, and engine power.

### Abstract

The "position" errors of the static systems of 10 service airspeed installations including static-pressure vents on the nose and rear section of the fuselage and pitot-static tubes mounted on the wing, the vertical tail, and the fuselage nose are presented. Tests were conducted at speeds between the stalling speed and 260 miles per hour for four flight conditions. Calibrations are analyzed to show variation of static-pressure error with position of static source, angle of attack, flap setting, and engine power.